ORGANOMETALLICS

Article

pubs.acs.org/Organometallics

A Thermodynamic Analysis of Rhenium(I)−Formyl C−H Bond Formation via Base-Assisted Heterolytic H_2 Cleavage in the Secondary Coordination Sphere

Thomas S. Teets, Jay A. Labinger,* and John E. Bercaw*

Arnold and Mabel Beckman Laboratories of Chemical Synthesis, California Institute of Technology, Pasadena, California 91125, United States

Supporting Information

ABSTRACT: Conversion of synthesis gas, a mixture of carbon monoxide and hydrogen, into value-added $C_{n\geq 2}$ products requires both C−H and C−C bond-forming events. Our group has developed a series of molecular complexes, based on group 7 (manganese and rhenium) carbonyl complexes, to interrogate the elementary steps involved in the homogeneous hydrogenative reductive coupling of CO. Here, we explore a new mode of H_2 activation, in which strong bases in the secondary coordination sphere are positioned to assist in the heterolytic cleavage of H_2 to form a formyl C−H bond at a rhenium-bound carbonyl. A series of cationic rhenium(I) complexes of the type $[Re^{I}(P{\sim}B{:}\text{-}\kappa_1\text{-}P)(CO)_5]^n$ (n = 0, +1), where P∼B: is a phosphine ligand with a tethered strong base, are prepared and characterized; measurement of their protonation equilibria demonstrates a pronounced attenuation of the basicity upon coordination. Formyl complexes supported by these ligands can be prepared in good yield by hydride delivery to the parent pentacarbonyl complexes, and several of the free-base formyl complexes can be protonated, generating observable $[Re^{I}(P{\sim}BH\text{-}\kappa_1\text{-}P)(CHO)(CO)_4]^n$ complexes. Intramolecular hydrogen bonding is evident for one of the complexes, providing additional stabilization to the protonated formyl complex. By measuring both the hydricity of the formyl, ΔG°_{H-}, and its pK_a, the overall free energy of H_2 cleavage is calculated from an appropriate cycle and found to be thermodynamically uphill in all cases (in the best case by only about 8 kcal/mol), although significantly dependent upon the properties of the supporting ligand.

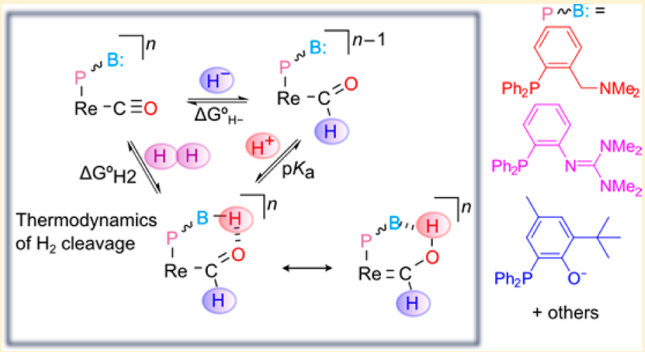

INTRODUCTION

Synthesis gas, or syngas, a mixture of carbon monoxide and hydrogen, can be derived from coal, biomass, or methane and is the key intermediate in the indirect conversion of these abundant, low-value natural resources into valuable fuels or commodity chemicals.[1] The best-known method for upgrading syngas is the Fischer−Tropsch process, which converts syngas into a complex mixture of hydrocarbon products.[2] The Fischer−Tropsch process traces its origins to over 80 years ago,[3] but to this day continued improvements are sought, primarily aimed at the development of more active catalysts[4] with narrower hydrocarbon distributions,[5] as well as modified systems that are selective for oxygenated products.[6] Experimental[7] and computational[8] studies on heterogeneous synthesis gas conversion catalyses have proliferated in recent years, leading to enhanced understanding of catalyst performance and selectivity.

A complementary strategy for converting syngas into more valuable products is homogeneous catalysis, which offers the potential of higher selectivity, milder operating conditions, and improved mechanistic understanding owing to the wealth of solution-phase techniques available for interrogating the structure, bonding, and energetic profiles of key reaction intermediates.[9] There are some examples of homogeneous catalytic synthesis gas conversion, with product selectivities that can favor $C_{n\geq 2}$ hydrocarbons[10] or alcohols,[11] depending on the choice of catalyst and operating conditions. However, to date homogeneous catalysts are not used industrially, and most of the focus with molecular species has been on modeling and studying proposed reaction intermediates. Earlier examples include studies on the formation, properties, and reactivity of metal formyl and related oxycarbene complexes, many of which are stable enough to be isolated;[12] in some cases carbon−carbon bond formation was observed upon reduction of metal-bound CO with hydride equivalents.[13] C−C bond formation was also modeled by studying the migratory insertion of CO into metal−alkyls, which can be promoted by Lewis or Brønsted acidic additives.[14]

In these early examples, strong hydride donors were used to form the C−H bond, and the Lewis acid additives that promoted C−C bond formation typically also resulted in the

Received: August 12, 2013
Published: October 3, 2013

   dx.doi.org/10.1021/om400810v | Organometallics 2013, 32, 5530−5545

formation of strong bonds between the Lewis acid and the acyl oxygen (perhaps better described as a stabilized oxycarbene in these cases). Practical application would require the use of H_2 (or hydride equivalents derived from H_2) to form the C−H bond and the use of milder Lewis acids to promote C−C bond formation. In recent years, advances in both of these areas have been made, by both our group and others. Noteworthy achievements include the use of secondary-coordination-sphere alkylborane Lewis acids to assist in heterolytic H_2 cleavage and C−C bond formation at rhenium carbonyl complexes;[15] employing main group frustrated Lewis pairs (FLPs) for homogeneous, stoichiometric CO hydrogenation and C−O bond cleavage;[16] reductive coupling of CO at an iron complex with participation from the supporting ligand;[17] and demonstrations that milder Lewis acids such as zinc(II) and calcium(II) can promote C−C bond formation by migratory insertion.[18] In spite of the fundamental advances described in these previous reports, several limitations remain. In the systems employing borane Lewis acid promoters, strong B−O bonds preclude product release and catalytic turnover, and the later examples that use milder Lewis acids also result in the formation of strong bonds between the rhenium center and charge-compensating halide ions that accompanied the Lewis acid, which could not be broken in a catalytically relevant fashion.

In this work, we examine a new approach for H_2 cleavage and formyl C−H bond formation, inspired in part by the reports of C−H bond formation mediated by H_2 activation at FLPs, where the resulting borohydride transfers hydride to CO. The latter demonstrate that prior activation of H_2 at a transition metal center, long thought to be a requisite, is in fact not necessary; perhaps the intermediacy of the borohydride can be bypassed as well? We envisioned a system in which a Brønsted base, positioned in the secondary coordination sphere of a metal carbonyl complex, assists in heterolytic H_2 cleavage, delivering hydride directly to a carbonyl carbon and simultaneously generating the conjugate acid of the appended base, which should be able to hydrogen bond with the resultant formyl oxygen and thus stabilize the product.

Obviously, the viability of this approach depends upon both kinetic and thermodynamic constraints. There is no good way to assess the former other than actually demonstrating a successful instance; but the thermodynamics, which depend on both the acid−base properties of the pendant group and the hydricity of the metal formyl, can be assessed by an appropriate combination of observables. As shown in Scheme 1, the desired overall reaction can be decomposed into a thermodynamic cycle with three elementary steps. The first step, (a), is the hydride-accepting free energy of the formyl, which is the negative of the formyl's hydricity, ΔG°_{H-}. The hydricities of several formyl complexes have been tabulated, and they range between 40 and 55 kcal/mol.[19] The free energy of reaction (b) depends on the pK_a of the rhenium formyl, with a multiplier to convert from unitless pK_a to kcal/mol; implicit in the measured pK_a is a contribution from hydrogen bonding between the formyl oxygen and the acidic proton, if present. Finally, to close the thermodynamic cycle, the free energy for heterolytic H_2 cleavage is included, which has been determined to be 76.0 kcal/mol in acetonitrile,[19] the solvent of choice for these studies. The overall free energy for H_2 cleavage, which is the sum of the energies for reactions (a)−(c) in Scheme 1, is abbreviated as ΔG°_{H2} herein. It should also be noted that the thermodynamic cycle can be written in a different way, starting

Scheme 1. Thermodynamic Cycle for Heterolytic H_2 Cleavage

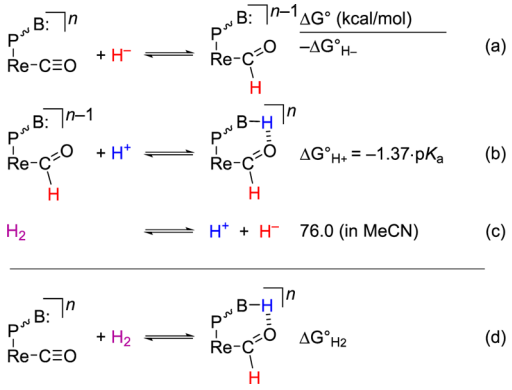

with protonation of the carbonyl complex and then addition of hydride to generate the formyl. This leads to the same overall reaction, but in practice the sequence outlined in Scheme 1 is more practical for measuring the overall reaction thermodynamics, as discussed later.

Rhenium(I) pentacarbonyl complexes of the type $[Re^I(P{\sim}B{:}\text{-}\kappa_1\text{-}P)(CO)_5]^n$ (n = 0, +1), where P∼B: is a phosphine ligand with an appended strong base, were chosen as the platform for the examination of these thermodynamic considerations. We report here the synthesis and reactivity of rhenium pentacarbonyl complexes with six different base-appended supporting ligands. In all cases, we were able to obtain complexes with exclusive ligation through phosphorus, leaving the base free, and to measure the pK_a of the protonated species. In several cases we have been able to generate the target structures, $[Re^I(P{\sim}BH\text{-}\kappa_1\text{-}P)(CO)_4(CHO)]^n$, by sequential reaction with strong hydride donor and weak acid, and determine their free energies of formation from the parent pentacarbonyl complex and H_2 using the thermodynamic cycle of Scheme 1. Unfortunately, all these values are unfavorable (in the best case by only about 8 kcal/mol), due largely to a very substantial attenuation of the basicity upon coordination, the extent of which depends on the precise structure of the ligand. Consistent with those findings, none of the complexes $[Re^I(P{\sim}B{:}\text{-}\kappa_1\text{-}P)(CO)_5]^n$ are reactive toward H_2. Nonetheless, the thermodynamic parameters and other results obtained in this work provide a useful framework and design criteria for this as well as related, potentially useful transformations.

RESULTS

Synthesis of Phosphine Ligands. Chart 1 presents the phosphine ligands that have been studied here, with the

Chart 1

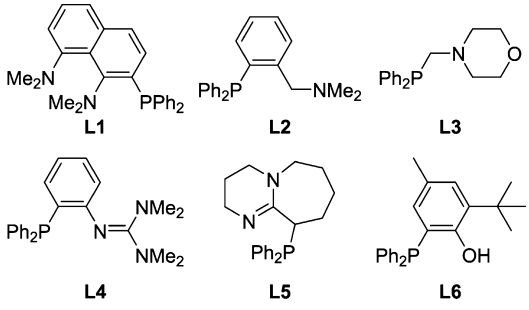

dx.doi.org/10.1021/om400810v | Organometallics 2013, 32, 5530−5545

abbreviations that will be used throughout. All ligands feature a diphenylphosphine ligating group with an appended basic unit. Most of the ligands in Chart 1 are described in the literature. Proton Sponge-substituted ligand **L1**,[20] *N*,*N*-dimethylbenzylamino-substituted **L2**,[21] and morpholine-substituted **L3**[22] were prepared as previously outlined. The ligand **L5**, which features the strong bicyclic base 1,8-diazabicyclo[5.4.0]undec-7-ene (DBU), has also been prepared,[23] but we opted for an alternate route whereby DBU was selectively lithiated at the 6-position[24] with *tert*-butyllithium, followed by addition of Ph_2PCl to install the diphenylphosphino substituent. Substituted phenol ligand **L6** (the protonated form of this ligand) was also prepared by a modified procedure: we lithiated the 2-bromo-substituted MOM-protected phenol precursor, whereas previous reports of this class of ligand begin their syntheses with direct C−H lithiation of the protected phenol precursor.[25,26]

The only new ligand described in this study is **L4**, which contains a 2-phenyl-1,1,3,3-tetramethylguanidine base. **L4** was accessed by a standard method for preparing mixed triarylphosphines (Scheme 2): the brominated precursor 2-

Scheme 2. Synthesis of L4

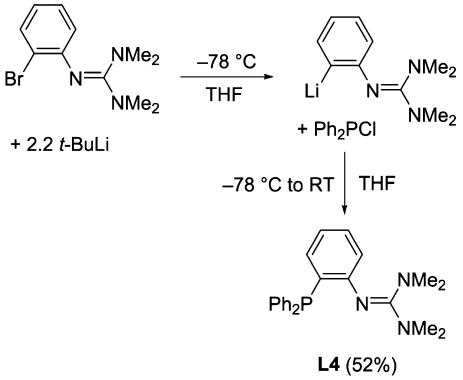

(2′-bromophenyl)-1,1,3,3-tetramethylguanidine[27] was lithiated at −78 °C via lithium−halogen exchange with *tert*-butyllithium, and addition of Ph_2PCl gave the desired product **L4**, which was isolated in 52% yield in gram quantities and found to be air-stable.

Synthesis of Protonated Ligands. Ligands **L1**−**L5** are all protonated at nitrogen upon addition of acid. Tetrafluoroborate salts of the ligands (abbreviated **(LxH)(BF$_4$)**, where "**x**" is the numerical designation for the ligand) were prepared as stable solids by treating the free-base ligand with HBF_4. **(L1H)(BF$_4$)** was prepared in EtOH by a previously reported procedure,[20] whereas the remaining ligands were protonated by $HBF_4{\cdot}Et_2O$ in aprotic solvents. Good yields of the desired salts were obtained, and all spectroscopic, mass spectrometric, and combustion analyses indicate monoprotonation, with no additional protonation at phosphorus or other available heteroatoms. In addition, the solid-state structure of **(L5H)(BF$_4$)** was determined by X-ray crystallography and is shown in Figure S1 of the Supporting Information. The N−H hydrogen atom was located in the difference map, and the presence of a hydrogen-bonding interaction with the BF_4^- counteranion is evident.

Synthesis and Properties of Cationic [Re^I(P∼B:-κ_1-P)(CO)$_5$]$^+$ Complexes. Reactions between neutral rhenium(I) starting materials $Re^I(CO)_5Br$ or $[Re^I(CO)_4(\mu\text{-}Br)]_2$ and ligands **L1**−**L5** typically result in κ_2-P,N complexes as major products, as a result of ligand substitution occurring at a similar rate to chelation. The desired κ_1-P complexes are accessible using more reactive cationic rhenium starting materials, which allow for milder conditions. Scheme 3 summarizes the general

Scheme 3. Synthesis of Cationic Rhenium Pentacarbonyl Complexes, with Isolated Yields in Parentheses

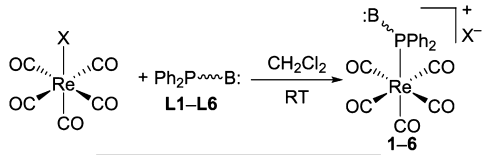

1: Ph_2P∼B:= **L1**; X = BF_4 (78%)
2: Ph_2P∼B:= **L2**; X = OTf (70%)
3: Ph_2P∼B:= **L3**; X = BF_4 (82%)
4: Ph_2P∼B:= **L4**; X = BF_4 (93%)
5: Ph_2P∼B:= **L5**; X = BF_4 (N/A)[a]
6: Ph_2P∼B:= **L6**; X = BF_4 (85%)

[a] Product not isolated

synthesis of these compounds. The labile rhenium(I) starting material $Re^I(CO)_5(FBF_3)$[28] showed the greatest utility, and in combination with **L1** and **L3**−**L6** in CH_2Cl_2 gave the desired complexes in good yields. Complex **5**, $[Re^I(\mathbf{L5}\text{-}\kappa_1\text{-}P)(CO)_5](BF_4)$, was observed as the major product in crude reaction mixtures, but could not be isolated in pure form due to contamination with the corresponding κ_2-P,N complex (vide infra). For ligand **L2**, reaction with $Re^I(CO)_5(FBF_3)$ gave a complex mixture of products, tentatively attributed to unselective binding of rhenium by phosphorus and nitrogen, but treatment with $Re^I(CO)_5(OTf)$ gave gradual conversion (1 week) to the desired complex $[Re^I(\mathbf{L2}\text{-}\kappa_1\text{-}P)(CO)_5](OTf)$ (**2**) in good yield.

In solution, the κ_1-P coordination mode is most readily discerned from the $^{31}P\{^1H\}$ NMR chemical shift, and from the $\tilde{\nu}_{C\equiv O}$ region of the IR spectra. The $^{31}P\{^1H\}$ NMR spectra for all complexes show singlets, in some case quite broad (fwhm ∼30−120 Hz), near 0 ppm (vs D_3PO_4). Similar features have been observed for other phosphine-ligated rhenium pentacarbonyl cations.[15c,18] In addition, the solution IR features of complexes **1**−**6**, where three IR-active CO stretching modes are evident, establish a C_{4v} geometry and match closely with other phosphine-ligated rhenium pentacarbonyl complexes.[29]

Solid-state structures of complexes **1**−**4** and **6** have all been determined by X-ray crystallography. The structure of **4**, representative of the series, is shown in Figure 1, with the remaining structures shown as Figures S2−S5 in the Supporting Information. The structures are unremarkable in most aspects, with bond angles all very close to 90°, as expected for a C_{4v}, axially elongated pseudo-octahedral structure. The Re−P bond distances are just under 2.5 Å, with Re−C distances all very near 2.0 Å. In addition, the distances between the tethered basic heteroatom and the rhenium center are all quite long; even the shortest such distance, 3.4840(7) Å between Re(1) and the phenolic O(6) in the structure of **6**, is much too long to be considered even a weak interaction.

Complexes **1**−**3** and **6** are indefinitely stable at room temperature in either dichloromethane or acetonitrile solution. However, complexes **4** and **5** do gradually decompose to their respective κ_2-P,N complexes when held at room temperature in solution. In the case of guanidine-substituted **4**, the decomposition is quite slow, occurring with a half-life on the

dx.doi.org/10.1021/om400810v | *Organometallics* 2013, 32, 5530−5545

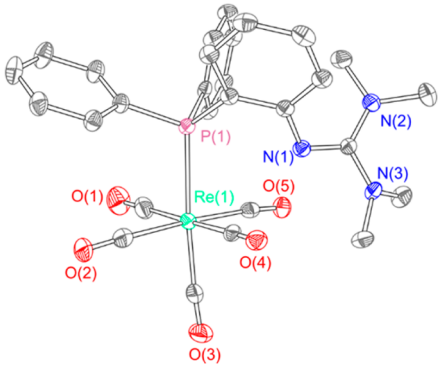

Figure 1. X-ray crystal structure of **4**, with thermal ellipsoids drawn at the 50% probability level. Hydrogen atoms and the BF_4^- counteranion are omitted for clarity.

order of several days, and multiple products are present, as judged by NMR. For **5**, with the DBU-substituted phosphine ligand, chelation is comparatively more rapid, occurring with a half-life of ca. 12 h at room temperature, such that complete conversion is noted within 60 h. The decomposition of complex **5** is outlined in Scheme 4, with the exclusive product

Scheme 4. Decomposition of 5 to 7

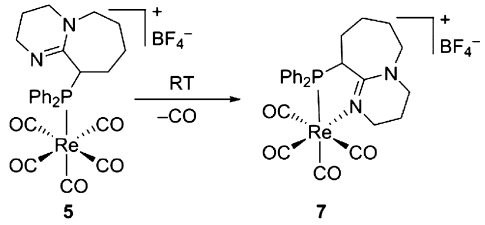

identified as $[Re^I(\mathbf{L5}\text{-}\kappa_2\text{-P,N})(CO)_4](BF_4)$ (**7**). The broad $^{31}P\{^1H\}$ resonance of **5** occurs at 1.3 ppm in dichloromethane, shifting downfield to 23.4 ppm and sharpening considerably in **7**. The IR spectrum of **7** is indicative of a pseudo-C_s coordination geometry brought on by chelation. In pentacarbonyl complex **5**, three CO stretching frequencies are observed, at 2151, 2091, and 2050 cm^{-1}, whereas in **7** four CO stretching frequencies are observed, occurring at significantly lower energy (2109, 2020, 2006, and 1968 cm^{-1}), on account of the more electron-rich rhenium center. And finally, complex **7** shows enhanced crystallinity relative to **5**, allowing its structure to be unambiguously obtained by X-ray crystallography. The structure of the cation is shown in Figure 2, which clearly shows the connectivity that was anticipated from the above-mentioned spectroscopic analyses. The P(1)−Re(1)−N(1) chelate angle is observed to be 75.70(8)°.

Acid/Base Chemistry of Rhenium Complexes. With complexes **1**−**6** in hand, we sought to explore their acid/base chemistry. Complexes **1**−**5**, which feature neutral nitrogenous tethered bases, can be protonated at the basic nitrogen to deliver dicationic complexes **8**−**12**. As summarized in Scheme 5, complexes **8**−**11** were prepared by addition of $HBF_4{\cdot}Et_2O$ to dichloromethane solutions of the corresponding $[Re^I(\mathbf{Lx})(CO)_5]^+$ complex. The desired dicationic $[Re^I(\mathbf{LxH})(CO)_5]^{2+}$ precipitated from solution and could be isolated in high yield. Owing to the inability to cleanly isolate DBU-substituted complex **5**, the complex $[Re^I(\mathbf{L5H})(CO)_5](BF_4)_2$ (**12**) was prepared by direct reaction of $(\mathbf{L5H})(\mathbf{BF_4})$ with $Re^I(CO)_5(FBF_3)$ at 50 °C in CH_2Cl_2 (Scheme 6). Once

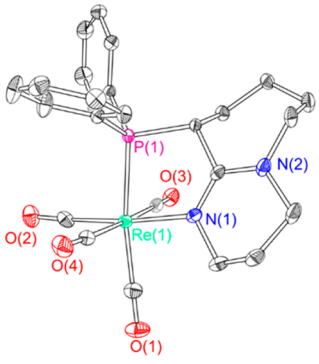

Figure 2. X-ray crystal structure of **7**, with thermal ellipsoids drawn at the 50% probability level. Hydrogen atoms and the BF_4^- counteranion are omitted.

Scheme 5. Synthesis of Protonated Rhenium Complexes 8−11

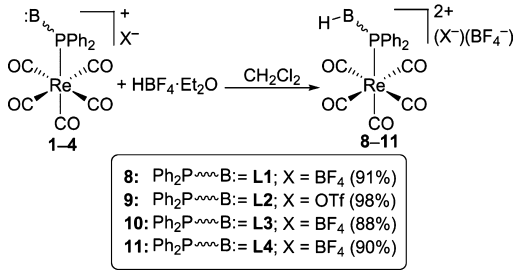

isolated, complexes **8**−**12** were soluble and indefinitely stable in acetonitrile solution, with no evidence for decomposition over prolonged time periods.

Scheme 6. Synthesis of Complex 12

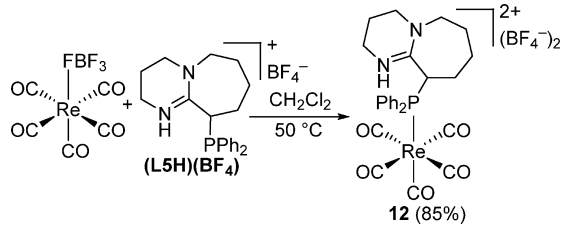

Several characteristic spectroscopic features distinguish complexes **8**−**12**. The $^{31}P\{^1H\}$ NMR spectra are shifted upon protonation, downfield for **8**, **11**, and **12** and upfield for **9** and **10** relative to their free-base analogues, but in all cases still in a spectral region characteristic of rhenium κ_1-P ligation. In the ^1H NMR spectra, the N−*H* resonance is unambiguously located in each case. The IR spectra in the $\tilde{\nu}_{C\equiv O}$ region are quite similar to those of complexes **1**−**5**, with hypsochromic shifts on the order of 5 cm^{-1}, reflecting a slight decrease in electron density at the metal center brought on by protonation.

The crystal structures of **8**, **9**, **11**, and **12** were determined, and that of **11** is shown in Figure 3 as a representative example. The coordination geometries about the rhenium centers are minimally perturbed relative to the structures of the unprotonated complexes, showing nearly identical bond lengths and angles. In each case the N−H hydrogen atom was located in the difference map and is oriented in such a manner to permit hydrogen bonding to a nearby counteranion. Analysis of the hydrogen bonding interactions in **8**, **11**, and **12** shows a

dx.doi.org/10.1021/om400810v | *Organometallics* 2013, 32, 5530−5545

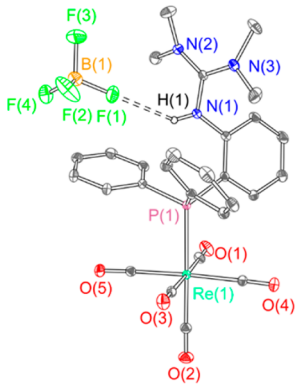

Figure 3. X-ray crystal structure of **11**, drawn at the 50% probability level. Carbon-bound hydrogen atoms, the CH_2Cl_2 solvent molecule, and the outer-sphere BF_4^- counteranion are omitted.

single-point hydrogen bond between the acidic proton and a fluorine atom of the BF_4^- counterion; this is true even for **8**, in which the proton is "chelated" by Proton Sponge via an intramolecular hydrogen bond. Complex **9** crystallized as a mixed OTf^-/BF_4^- salt, with preferential hydrogen bonding between the N−H proton and the triflate counterion. Elemental analysis confirms that **9** is also isolated as a mixed salt in the bulk sample.

Conditions were also sought to deprotonate complex **6**, to expose a strongly basic phenoxide unit in the vicinity of the rhenium center. Treatment of **6** with a sufficiently strong base, such as DBU, results in quantitative formation of the zwitterionic complex $Re^I(\mathbf{L6}^-\text{-}\kappa_1\text{-P})(CO)_5$ (**13**), which was identified spectroscopically. Scheme 7 summarizes the preparation and decomposition of **13**. The most identifying NMR feature for **13** is the $^{31}P\{^1H\}$ signal, which shifts downfield from that of **6** (−4.6 to 1.8 ppm) but is still diagnostic of a κ_1-P complex. In the ^1H NMR spectrum, the resonance for the aryl proton ortho to phosphorus shifts upfield dramatically, from 6.82 ppm to 6.06 ppm, and no O−*H* signal is detected, both of which are suggestive of deprotonation of **L6** to reveal a phenoxide. And finally, the IR spectrum shows three CO stretches (2100, 2074, 1996 cm^{-1}), consistent with a C_{4v} geometry and at substantially lower frequencies than those of **6** (2157, 2102, 2048 cm^{-1}).

Scheme 7. Synthesis and Decomposition of 13

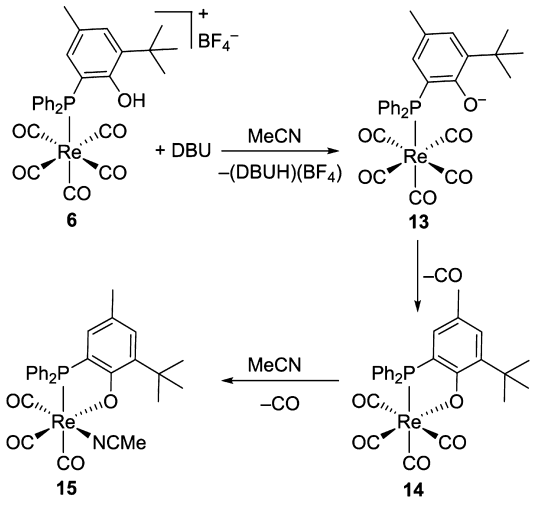

Complex **13** decomposes with a half-life of ca. 3 h at room temperature in acetonitrile, via a two-stage process. A metastable intermediate species, identified as $Re^I(\mathbf{L6}^-\text{-}\kappa_2\text{-P,O})(CO)_4$ (**14**), gives way over longer time periods to $Re^I(\mathbf{L6}^-\text{-}\kappa_2\text{-P,O})(CO)_3(NCMe)$ (**15**), which is confirmed as the facial isomer from the downfield CO $^{13}C\{^1H\}$ NMR features. Complex **14** is identified by its $^{31}P\{^1H\}$ NMR resonance at 25.6 ppm in CD_3CN, suggestive of κ_2-P,O ligation, and is the major product when **13** is heated in CH_2Cl_2. Complex **15**, which forms as the dominant product within 24 h in MeCN at 80 °C from a solution of **13**, is identified by a $^{31}P\{^1H\}$ NMR shift of 33.2 ppm in CD_3CN. An isolated sample of **15** shows a ^1H NMR signal at 0.00 ppm in C_6D_6 for the bound MeCN ligand, with weak (1.4 Hz) coupling to ^{31}P; when dissolved in CD_3CN, the NMR spectrum shows one equivalent of free CH_3CN.

pK_a Values of Ligands and Rhenium Pentacarbonyl Complexes. Table 1 summarizes the quantitative acid/base properties of the free ligands and their rhenium pentacarbonyl complexes, measured in acetonitrile. The values were determined by establishing equilibria with acids or bases of known strength, measuring equilibrium concentrations by NMR, and combining the measured equilibrium constant with the known pK_a via Hess's law to determine the unknown pK_a. The free ligand pK_a values are largely in line with those of the corresponding unsubstituted base, though it is worth noting that for ligands **4**−**6** the observed pK_a values are ca. 1−1.7 pK_a units smaller than those of the corresponding unsubstituted bases 2-phenyl-1,1,3,3-tetramethylguanidine (pK_a = 20.6),[30] DBU (pK_a = 24.34),[31] and phenol (pK_a = 29.14),[32] respectively.

Table 1. Summary of Acetonitrile pK_a Values for Ligands and Rhenium Pentacarbonyl Complexes

ligand	pK_a	complex	pK_a
L1H$^+$	18.24(2)[a]	**8**	11.02(5)
L2H$^+$	18.0(2)	**9**	13.00(3)
L3H$^+$	17.4(2)	**10**	5.7(2)
L4H$^+$	19.57(1)	**11**	13.09(4)
L5H$^+$	22.62(2)	**12**	13.34(4)
L6	28.17(5)	**6**	16.5(1)

[a]From ref 20.

For rhenium complexes **1**−**5** and **13**, the basicity is attenuated substantially compared to the free ligand. In terms of ΔpK_a, the smallest attenuation is observed for complex **2**, which also has the largest spacer length between the basic atom and the ligating phosphorus, with four carbon atoms separating the two. The largest decreases in basicity occur for **3**, which has only a methylene spacer between the phosphine and the morpholine base, and for substituted-phenolate complex **13**, where the anionic oxygen of the zwitterion suffers a nearly 12 order-of-magnitude decrease in basicity relative to the free phosphinophenolate **L6**$^-$. For complexes **1** and **4**, which contain three-carbon aromatic spacers between the neutral nitrogenous base and the phosphine, intermediate pK_a decreases of 7.22 and 6.48 are observed, respectively. Complex **5**, which has a three-carbon nonaromatic spacer between phosphine and basic nitrogen, shows a decrease in pK_a of 9.28 units.

Synthesis of Rhenium(I) Formyl Complexes. Complexes **1**−**5** and **13** are unreactive toward H_2, at room

dx.doi.org/10.1021/om400810v | *Organometallics* 2013, 32, 5530−5545

temperature and pressures up to 3 atm. To assess the thermodynamics of H_2 cleavage, as outlined in Scheme 1, we sought conditions to prepare the neutral formyl complexes, which would allow a comprehensive study of their ΔG°_{H-} and pK_a to calculate the overall thermodynamics. We found that the anionic tungsten(0) hydride complex (PPN)[*cis*-W^0(H)(P(OMe)$_3$)(CO)$_4$] (**W−H**), first described by M. Darensbourg and co-workers[33] and later utilized by DuBois et al.[34] to prepare a Cp*-ligated rhenium formyl, proved to be an effective hydride reagent for rapidly generating high yields of the neutral formyl complexes **16**−**20**, as summarized in Scheme 8, with

Scheme 8. Synthesis of Rhenium Formyl Complexes 16−20

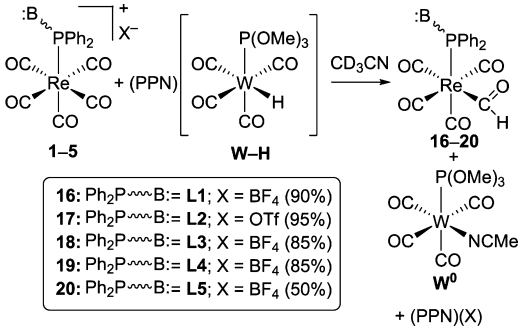

approximate yields from NMR integration shown. Within minutes of mixing equimolar amounts of pentacarbonyl complexes **1**−**5** and **W−H** in acetonitrile all spectral data are consistent with the formation of unstabilized rhenium formyl complexes *cis*-Re^I(**Lx**)(CHO)(CO)$_4$ (**16**−**20**). In all instances, the tungsten-containing product is identified as *cis*-W^0(P(OMe)$_3$)(NCMe)(CO)$_4$ (**W^0**), identified by its NMR features and with IR spectral features nearly matching a closely related complex.[35] The spectral features attributed to **W^0** show no dependence on the identity of the rhenium formyl, confirming an absence of interaction between the formyl oxygen and the tungsten center, which has been previously been observed.[34]

In contrast to the above, hydride transfer from **W−H** to phenol-substituted complex **6** was not observed. With a single equivalent of **W−H**, only deprotonation was observed, giving zwitterion **13** as the sole product. With two equivalents, **13** was again observed, along with an equivalent of unreacted **W−H**, with no hydride transfer on the time scale of the decomposition of **13**. However, the anionic formyl complex Li[*cis*-Re^I(**L6**$^-$)(CHO)(CO)$_4$] could be generated from **6** by treatment with two equivalents of $LiHBEt_3$ (Scheme 9).

Rhenium formyl complexes **16**−**21** were not isolated, owing to the difficulty of separating them from their respective byproducts and their instability under vacuum, though spectral

Scheme 9. Synthesis of Anionic Borane-Stabilized Formyl Complex 21

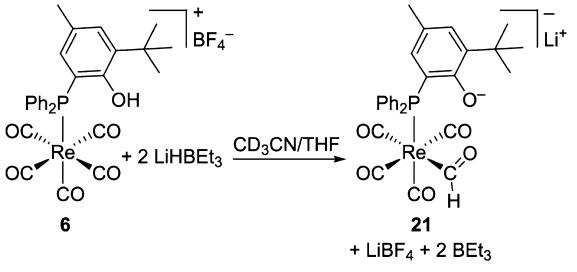

monitoring of reactions shows that they are formed in moderate to excellent yields and decompose with half-lives of two hours or more. Table 2 summarizes the key spectral

Table 2. Summary of Spectral Characteristics of Rhenium Formyl Complexes[a]

complex	$\delta_{CHO}(^1H)$ (ppm)	$\delta_{CHO}(^{13}C)$ (ppm)	$^2J_{CP}$ (Hz)	$\nu_{C=O}$ (cm^{-1})
16	14.91	259.4	9.1	1590
17	14.98	259.6	9.4	1590
18	15.14	259.2	10.4	1590
19	14.86	260.0	9.6	1590
20	15.16	ND[b]	ND[b]	1589
21	15.14	274.9	12.0	1584

[a]Recorded in acetonitrile. [b]Not determined on account of the low yield and poor stability of complex **20**.

characteristics of rhenium formyl complexes **16**−**21**. In general the spectral characteristics attributable to the formyl group show little dependence on the identity of the supporting phosphine. In the ^1H NMR spectra, the characteristic formyl C−*H* resonance appears near 15 ppm, whereas in the $^{13}C\{^1H\}$ NMR the formyl carbon resonates close to 260 ppm, substantially downfield of the carbonyl resonances. For complex **21**, the $^{13}C\{^1H\}$ NMR resonance appears further downfield, at 274.9 ppm, likely due to the negative charge and/or an interaction with BEt_3 or Li^+ leading to more carbene character.[12b] Further support for an interaction with BEt_3 comes from the ^1H NMR spectrum, where the resonances for BEt_3 are shifted upfield relative to those of free BEt_3. It is also possible that the basic phenoxide oxygen interacts with BEt_3 or Li^+, though NMR evidence for this this possibility is not conclusive. The ^{13}C NMR shift of the phenoxide C1 remains far downfield (169.3 ppm), and the ^1H NMR resonance for the aryl proton ortho to phosphorus is very far upfield (5.82 ppm), both of which are suggestive of considerable phenoxide character (see Experimental Section). In all complexes, couplings of the formyl proton and carbon with the ^{31}P nucleus are quite small, ≤1.4 Hz for $^3J_{HP}$ and 9−10 Hz for $^2J_{CP}$, indicating a cis geometry. The C═O formyl stretch in the IR spectrum is essentially independent of the identity of the phosphine, appearing near 1590 cm^{-1} for **16**−**20** and at slightly lower energy (1584 cm^{-1}) for **21**. And finally, other spectral features attributed to the CO ligands are indicative of the altered coordination geometry and increase in electron density at the rhenium center; the three distinct $^{13}C\{^1H\}$ *CO* peaks in **16**−**19** are ca. 10−15 ppm downfield of the two observed resonances in pentacarbonyl complexes **1**−**5**, and the $\tilde{\nu}_{C\equiv O}$ IR spectral region shows four bands,[36] indicative of the decrease to approximate C_s symmetry and occurring at lower energies than those of the parent pentacarbonyl complexes.

Protonation of Formyl Complexes. Treatment of Proton Sponge-substituted formyl complex **16** with lutidinium tetrafluoroborate resulted in gradual formation, over a period of 45 min, of pentacarbonyl complex **1** and H_2, with no NMR evidence for a protonated formyl complex. Substituting the stronger acid anilinium tetrafluoroborate, or subjecting complexes **18** and **20** to similar treatments, likewise failed to produce an observable protonated formyl complex in appreciable yield. In contrast, treatment of complexes **17**, **19**, and **21** with weak acids gave protonated formyl complexes **22**−**24** as major products, which were spectroscopically observable. Optimum yields were obtained when the acid was added to

dx.doi.org/10.1021/om400810v | *Organometallics* 2013, 32, 5530−5545

thawing solutions of the formyl complex, which inhibited a side reaction where the acid directly reacted with the formyl directly to release H_2. Scheme 10 summarizes the protonation of formyl complexes **17**, **19**, and **21** to generate **22**–**24**.

Scheme 10. Protonation of Formyl Complexes 17, 19, and 21 to Generate 22–24, with Estimated NMR Yields in Parentheses

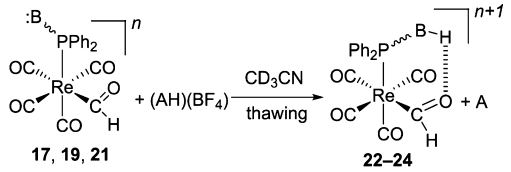

22: Ph_2P〰B: = **L2**; *n* = 0; A = pyridine (50%)
23: Ph_2P〰B: = **L4**; *n* = 0; A = 2,6-lutidine (70%)
24: Ph_2P〰B: = **L6**$^-$; *n* = –1; A = 2,6-lutidine (75%)

Complex **22** was formed only in moderate yields (~50%), and its poor stability and broad NMR features complicated characterization. Nevertheless, ^{1}H and ^{31}P{^{1}H} NMR spectra clearly indicated the formation of **22**. In the ^{1}H NMR spectrum, the formyl C*H*O resonance shifts downfield, from 14.98 ppm in **17** to 15.15 ppm in **22**, with considerable broadening in the latter. The ^{31}P{^{1}H} NMR signal of 13.0 ppm for protonated complex **22** is also distinct from that of the free-base precursor **17** (11.6 ppm). Once formed, complex **22** decomposes by loss of H_2, and within 6 h at room temperature it has completely given way to pentacarbonyl complex **2** as the major product. Neutral complex **24**, supported by phenol-based ligand **L6**, was formed in better yields (~75%) and had much more distinct spectroscopic features than those of complex **22**, but also suffered from poor stability. Initial NMR spectra after addition of 2,6-lutidinium tetrafluoroborate to a solution of **21** show complex **24** as the major species. Figure S9 shows the downfield region of the NMR spectra of **21** and **24**, showing the distinct change that occurs upon protonation. In the ^{1}H NMR spectrum, the formyl resonance shifts from 15.14 ppm in **21** to 14.82 ppm in **24**, and a distinct O–*H* singlet is present at 8.42 ppm. In the ^{31}P{^{1}H} NMR spectrum, the singlet at 5.6 ppm in **21** shifts to 7.6 ppm in **24**. It should be noted that BEt_3 is still present in these samples, likely interacting with the formyl and influencing the observed chemical shifts. In the IR spectrum, an apparent C═O formyl stretch for **24** is located at 1595 cm^{-1}, though other resonances in this region complicate this assignment. Complex **24** displays poor stability, undergoing nonspecific decomposition over the course of 1 h to a complex mixture of products.

Complex **23**, supported by the phenylguanidine-containing ligand **L4**, proved to be the most stable and amenable to characterization. Whereas the formyl C═O stretching region of the IR spectrum is obscured by ligand-based resonances, making it difficult to pinpoint the formyl stretch, multinuclear NMR spectroscopy clearly reveals **23** as the major product, obtained in 75% yield when a solution of **19** in thawing acetonitrile is treated with 2,6-lutidinium tetrafluoroborate. The ^{31}P{^{1}H} NMR spectrum shows a single resonance at 10.5 ppm, distinct from that of free-base precursor **19** (9.3 ppm). Even more telling are the changes to the ^{1}H and ^{13}C{^{1}H} NMR spectra that occur upon protonation of **19** to give **23**. In the downfield region of the ^{1}H NMR spectrum, Figure S10, the formyl resonance shifts from 14.86 ppm to 15.38 ppm, and a sharp N*H* resonance appears at 9.23 ppm. In the upfield region the N(CH_3)$_2$ resonance shifts downfield from 2.20 ppm in **19** to a much broader signal at 2.73 ppm in **23**. The downfield region of the ^{13}C{^{1}H} NMR spectrum is also diagnostic; the peak attributed to the formyl carbon shifts from 260.0 ppm in **19** to 269.4 ppm in **23**, whereas the CO carbons undergo a very slight, ca. 2 ppm upfield shift. Complex **23** is moderately stable in solution, decomposing over the course of ca. 30 h via dehydrogenation, which produces pentacarbonyl complex **4**, and decarbonylation, which produces protonated hydride complex **25**, as depicted in Scheme 11. Complexes **4** and **25**

Scheme 11. Decomposition Pathways for Protonated Formyl Complex 23

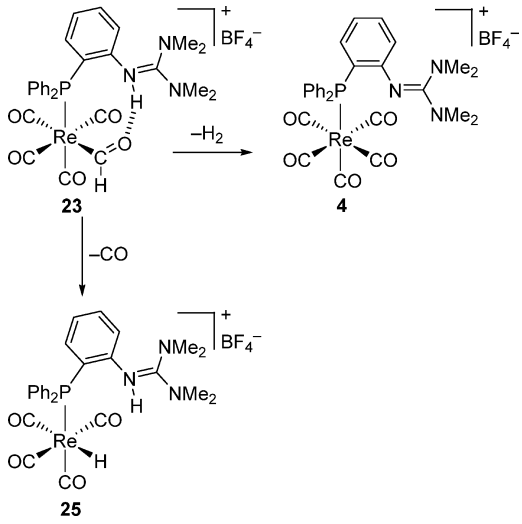

are present in a 2.3:1 ratio at the end of the reaction, suggesting that dehydrogenation occurs twice as fast as decarbonylation. Complex **25** is most readily identified by a ^{1}H NMR doublet at −5.51 ppm ($^2J_{HP}$ =20.4 Hz), suggestive of a hydride cis to the phosphine, and a singlet at 8.71 ppm for the N*H* proton, distinct from that of complex **23** and indicating that hydride complex **25** remains protonated upon decarbonylation.

pK_a's of Formyl Complexes. Using a method analogous to that described above for the pentacarbonyl complexes, the pK_a's of complexes **22**–**24** were determined in acetonitrile. For complex **22**, the pK_a was determined to be 14.4(1), by equilibration of free-base formyl **17** with 2,6-lutidinium. Consistent with this observation, addition of 4-dimethylaminopyridinium (DMAPH$^+$, pK_a = 17.95)[31] to neutral formyl complex **17** resulted in no evidence for proton transfer. The pK_a of **23** was determined by equilibration of **19** with DMAPH$^+$, with a value of 16.6(3) obtained. For **24**, the pK_a measurement was complicated by varying interactions of **21** and **24** with triethylborane, which causes changes in the equilibrium NMR shifts and interferes with the determination of the equilibrium concentrations. Nevertheless, it was observed that treatment of **21** with DMAPH$^+$ led to incomplete deprotonation of the acid, and by measuring the equilibrium populations of DMAP and DMAPH$^+$ an estimated pK_a of 17.7 was obtained for complex **24**. Consistent with this estimate, treatment of **21** with 2-(2′-tolyl)-1,1,3,3-tetramethylguanidinium (pK_a = 20.5)[30] left the NMR signals of **21** unperturbed, indicating no protonation.

dx.doi.org/10.1021/om400810v | *Organometallics* 2013, 32, 5530–5545

ΔG°_{H-} of Rhenium Formyl Complexes. The thermodynamic hydricities of rhenium formyl complexes **17** and **19** were determined by equilibration with group 10 hydride complexes. Reactions between the cationic carbonyl complexes **2** and **4** and the cationic group 10 hydride complexes are quite sluggish compared to the hydride transfer from the anionic complex **W−H**, making it difficult to judge if equilibrium has been reached before onset of decomposition of formyl complexes **17** and **19**. Fortunately, complexes **17** and **19** are the most stable of the formyl complexes studied here, persisting for days in solution. Treatment of **2** and **4** with $[Pt(H)(dmpe)_2](PF_6)$ (ΔG°_{H-} = 42.5 kcal/mol) leads to nearly quantitative hydride transfer; over the course of 8 h (**2**) or 14 h (**4**) the pentacarbonyl complexes are completely consumed, suggesting that ΔG°_{H-} for the formyl complexes is at least 2.5 kcal/mol greater. During these time frames decomposition of the formyl is observed to a minor extent, with the rhenium-hydride complex present at <20% relative to the formyl product in each case. Treatment with $[Pt(H)(depe)_2](PF_6)$ (ΔG°_{H-} = 44.2 kcal/mol) leads to much slower conversion, but low yields of formyls **17** and **19** are observed, as well as some of the rhenium-hydride decarbonylation products. In addition, combination of **2** or **4** and $[Ni^{II}(H)(dmpe)_2](PF_6)$ (ΔG°_{H-} = 50.9 kcal/mol) shows no sign of hydride transfer over the course of 24 h or longer, suggesting that ΔG°_{H-} for the formyl complexes is at least 2.5 kcal/mol smaller than that of the nickel-hydride reagent. Taken together, the results of the reactions with platinum- and nickel-hydride reagents allow us to determine that the ΔG°_{H-} for **17** and **19** are the same within experimental error, with values of 45(2) kcal/mol. In the case of anionic formyl **21**, an accurate value for ΔG°_{H-} could not be determined, since **21** can be generated only with borohydride reagents, and interaction of the formyl with the borane byproduct skews equilibrium measurements (also, ΔG°_{H-} for these hydride reagents have not been experimentally determined). However, the knowledge that **W−H** (ΔG°_{H-} = 37(2) kcal/mol)[34] is unable to transfer a hydride to complex **13** (vide supra) suggests that the ΔG°_{H-} for the anionic formyl complex **21** is ≲34(2) kcal/mol.

Complete Thermodynamics of H_2 Cleavage. By combining the ΔG°_{H-} values and pK_a values of the formyl complexes, the overall free energy of H_2 cleavage, ΔG°_{H2}, can be determined as outlined in Scheme 1. Table 3 summarizes the relevant thermodynamic parameters for the formation of protonated formyl complexes **22−24**. As seen from the values in Table 3, H_2 cleavage is unfavorable for all three complexes at standard conditions (1 atm H_2, 25 °C). The small difference between complexes **22** and **23** is due to the difference in pK_a between the two complexes, whereas the much larger ΔG°_{H2} value for complex **24** is a result of its much smaller ΔG°_{H-}.

Table 3. Thermodynamic Parameters for 22−24[a]

complex	ΔG°_{H-} (kcal/mol)	pK_a	ΔG°_{H2} (kcal/mol)
22	45(2)	14.4(1)	11(2)
23	45(2)	16.6(3)	8(2)
24	≲34(2)	∼17.7	≳17(2)

[a]Values for complex **24** are approximate, for reasons given in the text.

DISCUSSION

The cationic rhenium pentacarbonyl complexes **1−5** and **13**, containing six different tethered-base phosphine ligands with varying basic groups and spacers, constitute a platform for investigating the key intermediates in the proposed approach to homogeneous syngas conversion based on intramolecular base-assisted heterolytic H_2 activation. We have established conditions for avoiding the tendency of these ligands to coordinate in κ_2 fashion (Scheme 3), with the resulting κ_1-P complexes showing room-temperature stabilities of several hours or more. The IR spectra of the complexes suggest strongly electrophilic carbonyl ligands in **1−5**, with $\tilde{\nu}_{C\equiv O}$ values well above 2000 cm^{-1} in all cases, with little dependence on the identity of the supporting ligand. Furthermore, these stretching frequencies are nearly identical to analogous complexes supported by simple tertiary phosphines,[29] demonstrating that the electron-rich basic moieties of **L1−L5** do not influence the metal center substantially when bound in the κ_1-P mode. In zwitterion **13** the carbonyl stretching frequencies decrease substantially (ca. 50 cm^{-1}), reflecting the decreased electrophilicity in the neutral complex.

Complexes **1−5** can all be protonated to yield stable dicationic complexes **8−12**. The spectral properties of the protonated complexes suggest little change in the electronic properties of the metal center upon protonation of the pendant base; both the $^{13}C\{^1H\}$ NMR and IR spectral features associated with the carbonyl ligands are affected minimally, showing that the tethered base can engage in acid/base chemistry with little impact at the rhenium center. However, the converse is not at all true: measurement of the pK_a values of complexes **6** and **8−12** shows that coordination to rhenium results in a severe attenuation of the ligand's basicity, exhibiting decreases of 5−12 orders of magnitude for the cationic carbonyl complexes compared to the free ligands (Table 1). With this small set of complexes it is difficult to discern trends in the behavior; for example, the single methyl spacer in **3** and the aryl spacer in **13** both result in a ca. 12-pK_a-unit attenuation, but the same aryl spacer in **4** tempers the basicity by only ∼7 pK_a units. It seems likely that both the identity of the dangling base and the nature of the spacer between the base and the ligating group influence the pK_a of the bound ligand.

We envisioned the H_2-activation reaction outlined in Scheme 1 as proceeding through a similar mechanism to other known heterolytic H_2-cleavage reactions,[37] where in this case the CO π^* orbital, which is polarized toward carbon, is the acceptor orbital. In spite of many examples in the literature of H_2 cleavage to make transition metal or main-group hydrides, there are no examples of a metal-bound CO directly serving as the hydride acceptor in a H_2-cleavage reaction, but it is not obvious whether such a transformation is thermodynamically disfavored or merely kinetically difficult.

To obtain the thermodynamic parameters needed for the analysis of Scheme 1, it was important that the metal formyl complexes be free of any interaction with Lewis acidic species in solution, as these (which have been shown to occur on numerous occasions[12b,34,38]) would perturb the measured thermodynamics of the various elementary steps. For cationic complexes **1−5**, treatment with anionic complex **W−H** furnished neutral formyl complexes **16−20** in moderate to excellent yield, showing no interaction with the byproducts (the 18-electron complex *cis*-$W^0(P(OMe)_3)(NCMe)(CO)_4$ (**W^0**) and the weakly electrophilic cation PPN^+). The spectral characteristics attributed to the formyl and carbonyl groups in **16−20** are all quite similar to each other, once again showing that the supporting phosphine ligand has a minimal impact on the electronic properties of the rhenium center.

dx.doi.org/10.1021/om400810v | *Organometallics* 2013, 32, 5530−5545

Attempts to protonate neutral formyl complexes **16**–**20** with weak acids gave mixed results. In some cases, addition of acid resulted either in rapid H_2 generation, with no evidence for the desired product, or in complex, intractable product mixtures. In three cases, though, we were able to prepare protonated formyl complexes—which would be the products of the proposed heterolytic H_2 cleavage—by sequential addition of hydride and proton equivalents to the pentacarbonyl complexes. Amine-tethered complex **17** and anionic phenoxide-decorated complex **21** could both be protonated to give observable protonated formyl complexes **22** and **24**, respectively, though a combination of low yield (**22**) and poor stability (**24**) hindered complete spectroscopic analysis of these complexes. However, protonation of formyl complex **19**, supported by the novel guanidine-based ligand **L4**, gave protonated formyl complex **23**, which formed in good yields and was sufficiently stable for spectroscopic characterization. In particular, the $^{13}C\{^1H\}$ NMR spectrum of **23** is suggestive of intramolecular hydrogen bonding between the guanidinium moiety and the oxygen of the formyl: the resonance attributed to the formyl carbon shifts downfield from 260.0 ppm (**19**) to 269.4 ppm (**23**), which is indicative of enhanced carbene character in the formyl group.[12b,15a] Figure 4 illustrates two resonance structures of

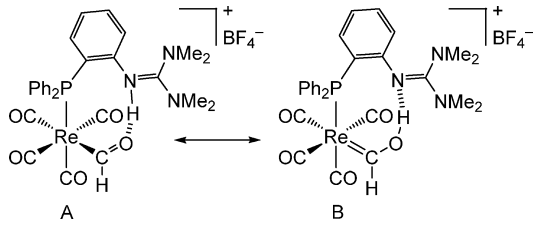

Figure 4. Contributing resonance structures for protonated formyl complex **23**.

23, and the sizable shift of the formyl $^{13}C\{^1H\}$ resonance relative to **19** indicates that hydroxycarbene structure **B** is an important contributor. Further support for intramolecular hydrogen bonding comes from the ^1H NMR spectra, where the sharp signals for the formyl C–*H* and the guanidinium N–*H* protons suggest rigidity, and the substantial broadening of the $N(CH_3)_2$ resonance in **23** relative to the sharp signal observed in **19** is reflective of a more hindered interchange between the two dimethylamino groups in the former.

Having established syntheses and spectral properties of the protonated formyl species, setting up equilibria utilizing weaker hydride reagents and acids allowed for the determination of the thermodynamic parameters ΔG°_{H-} and pK_a for the formyl complexes. The combination of these two parameters (Table 3) shows that, in all cases, the cleavage of H_2 is thermodynamically prohibited at the pressures of H_2 attainable in a laboratory setting. Consistent with those findings, complexes **1**–**5** and **13** are all unreactive toward H_2, up to 3 atm at room temperature in acetonitrile, while the putative products, the protonated base–formyl complexes (**22**–**24**), which could be synthesized by the alternate stepwise route in several instances (Schemes 8 and 10), all decompose (albeit rather slowly) by loss of H_2.

The last observation provides a small piece of encouragement: since loss of H_2 is the microscopic reverse of the target transformation, we know at least that there is no insurmountable kinetic barrier. Might it be possible to use the lessons learned here to design a system in which the thermodynamics become favorable? Our initial choices for study, the complexes of **L1**–**L5**, feature neutral nitrogenous bases whose pK_a's *should* have been high enough to promote heterolytic H_2 activation, given known ΔG°_{H-} values for similar formyl complexes. However, coordination to Re reduced their basicities by 5–12 orders of magnitude, enough to take them out of the range where H_2 cleavage was predicted to be favorable. This motivated pursuit of the phenoxide-based zwitterionic complex **13**, which was expected to—and does—show enhanced basicity compared to the cationic complexes, by several pK_a units (Table 1). Unfortunately, that change is accompanied by a substantial decrease in carbonyl electrophilicity, such that the ΔG°_{H-} is much smaller in magnitude, resulting in overall thermodynamics of H_2 cleavage by **13** to form complex **24** that are the most unfavorable of all. That was a somewhat surprising, and quite disappointing result: ΔG°_{H-} values for the two formyl complexes (**22** and **23**) for which good numbers could be measured are the same, 45(2) kcal/mol. The coincidence of these two values is consistent with the spectroscopic observations that suggested the properties of the rhenium-bound carbonyls do not depend significantly on the identity of the nitrogen-base tethered ligand. In contrast, switching to a phenoxide base does have a major unfavorable effect on the hydride-accepting properties of the carbonyls, presumably a consequence of the net change in overall charge. Clearly—and not so surprisingly—trying to improve thermodynamics by redesigning the system can result in trade-offs.

The simplest inference from these findings is that a ligand featuring a much stronger—but still neutral—appended base could improve the thermodynamics and possibly lead to a successful demonstration of the targeted heterolytic H_2 activation. However, the path forward is not so straightforward; while (unfunctionalized) bases meeting these criteria are available,[31] they do not appear readily amenable to attachment to phosphines or other ligands. Also, there will probably be additional factors governing the stability of the desired product, particularly the strength of intramolecular hydrogen bonding between the protonated base and the oxygen of the formyl, which may well depend on specific structure. For example, the pentacarbonyl complexes of ligands **L2** and **L4** have nearly identical acid/base properties (Table 1), whereas the corresponding formyl complexes exhibit significantly different pK_a values, 14.4(1) and 16.6(3), respectively, suggesting that the guanidinium unit in **23** may be better positioned to hydrogen bond with the formyl than is the trialkylammonium group in **22**. Another means of improving the overall thermodynamics of H_2 cleavage is to increase the hydricity (ΔG°_{H-}) of the formyl, which is 45(2) kcal/mol for **17** and **19**. On the basis of previously tabulated formyl hydricities, the analogous manganese(I) pentacarbonyl complexes ($\Delta G^\circ_{H-} \approx$ 50 kcal/mol) and complexes of the type $[Re^I(Cp)(CO)_2(NO)]^+$ (Cp = cyclopentadienyl, $\Delta G^\circ_{H-} \approx$ 55 kcal/mol) are better hydride acceptors than the rhenium complexes described here.[19] Manganese(I) pentacarbonyl complexes with base-appended phosphines, in particular **L4**, are currently being studied, and we are also looking to develop synthetic strategies for tethering a guanidine or other strong base onto rhenium(I)-cyclopentadienyl complexes. In spite of the thermodynamic challenges outlined herein, we continue to explore this approach for heterolytic H_2 cleavage, as well as other possibilities for using secondary coordination sphere interactions of ligand-appended Brønsted acids and bases to promote transformations of relevance to catalytic syngas conversion.

dx.doi.org/10.1021/om400810v | *Organometallics* 2013, 32, 5530–5545

EXPERIMENTAL SECTION

Materials. All reactions were executed in a glovebox filled with either N_2 or argon or on a Schlenk line under argon. Solvents were dried by passing through an alumina column using the method of Grubbs,[39] and deuterated NMR solvents were passed through a short column of alumina prior to use. CD_3CN was further dried by storing over molecular sieves. Hydrogen was passed through columns of molecular sieves and manganese oxide prior to delivery through a high-vacuum manifold. The ligands 1,8-dimethylamino-2-diphenylphosphinonapthalene (**L1**),[20] 2-diphenylphosphino-*N*,*N*-dimethylbenzylamine (**L2**),[21] and *N*-(diphenylphosphinomethyl)morpholine (**L3**)[22] were prepared as described in the literature. The tetrafluoroborate salt of **L1** (**(L1H)(BF$_4$)**) was also available by a previously described synthesis.[20] The sodium salt of **L6** was prepared as previously outlined for related ligands[40] and was used in the pK_a determination of **L6**. The ligand precursors 2-(2′-bromophenyl)-1,1,3,3-tetramethylguanidine[27] and methoxymethyl ether-protected 2-bromo-6-*tert*-butyl-4-methylphenol[41] were also obtained from literature routes. The rhenium(I) starting materials $Re^I(CO)_5(FBF_3)$[28] and $Re^I(CO)_5(OTf)$[42] (OTf = trifluoromethanesulfonate) were likewise prepared by published methods. Commercially available bases 2,6-lutidine, triethylamine, 2-chloroaniline, aniline, pyridine, and 1,8-diazabicyclo[5.4.0]undec-7-ene were purified by standard methods,[43] whereas 4-dimethylaminopyridine (DMAP) was used as received. The base 2-(2′-tolyl)-1,1,3,3-tetramethylguanidine was prepared by a modified literature procedure,[27] substituting toluene for benzene as the reaction solvent and heating to reflux. The tetrafluoroborate salts of 2,6-lutidine, aniline, and pyridine, and 2-(2′-tolyl)-1,1,3,3-tetramethylguanidine were obtained by treating a solution of the base in Et_2O with one equivalent of $HBF_4{\cdot}Et_2O$; the salts precipitated as white solids, which were deemed pure by ^{1}H NMR. The tetrafluoroborate salt of DMAP was prepared similarly, using MeCN as the solvent, and precipitating the product with Et_2O. Lithium triethylborohydride (Super Hydride) was obtained from Aldrich as a 1.0 M THF solution. The hydride reagents (PPN)[*cis*-$W^0(H)(P(OMe)_3)(CO)_4$][33] (**W−H**, PPN = bis(triphenylphosphine)-iminium), $[Pt^{II}(H)(diphosphine)_2][PF_6]$[44] (diphosphine = bis-(dimethylphosphino)ethane (dmpe), bis(diethylphosphino)ethane (depe)), and $[Ni^{II}(H)(dmpe)_2][PF_6]$[44] were prepared as previously described.

Physical Methods. ^{1}H and ^{31}P{^{1}H} NMR spectra were recorded on a Varian Mercury 300 spectrometer, operating at 300 MHz for ^{1}H acquisition and 121.5 MHz for ^{31}P acquisition. ^{13}C{^{1}H} NMR were recorded on a Varian Inova 500 spectrometer, operating at 125.7 MHz. ^{1}H and ^{13}C{^{1}H} spectra were referenced to solvent resonances, whereas ^{31}P NMR spectra were referenced to an external standard of 85% D_3PO_4. All NMR spectra were acquired at room temperature. For ^{13}C{^{1}H} NMR spectra of formyl complexes, the default decoupling frequency resulted in incomplete decoupling for the formyl resonance. Hence for all formyl complexes additional scans were recorded with the ^{1}H decoupling frequency centered at 15 ppm; the insets of the depicted ^{13}C{^{1}H} NMR spectra in the Supporting Information display the CO region of the spectrum recorded as such. IR spectra were recorded on a Nicolet 6700 spectrometer. Samples were housed in a solution cell with KBr windows and a 0.1 mm Teflon spacer. High-resolution mass spectrometry was executed on a JEOL JMS-600H high-resolution mass spectrometer operating in FAB+ mode with 3-nitrobenzyl alcohol as the matrix. Elemental analyses were performed by Midwest Microlab LLC.

Preparation of 2-(2′-Diphenylphosphinophenyl)-1,1,3,3-tetramethylguanidine (L4). A Schlenk flask was charged with 2-(2′-bromophenyl)-1,1,3,3-tetramethylguanidine (4.26 g, 15.8 mmol) dissolved in 50 mL of THF. The colorless solution was cooled in a dry ice/acetone bath, after which a pentane solution of *tert*-butyllithium (1.63 M, 21 mL, 34 mmol, 2.2 equiv) was added via cannula, effecting a color change to bright yellow. After stirring for 1 h while being kept cold, Ph_2PCl (3.48 g, 15.8 mmol, 1.00 equiv), diluted with 6 mL of THF, was added via cannula. The initially yellow solution was stirred for 2 h, at which time the cold bath was removed and the mixture allowed to warm to room temperature and stirred overnight, during which the color darkened to a deep red-brown color. Addition of 2 mL of methanol caused the color to fade to yellow. The volatiles were removed in vacuo, producing a yellow-orange residue. The remaining workup was performed in ambient atmosphere. The crude product was dissolved in 50 mL of CH_2Cl_2 and washed with 50 mL of water. The aqueous phase was extracted with an additional 50 mL of CH_2Cl_2, and the combined organic phases were dried over $MgSO_4$ and concentrated by rotary evaporation to leave an orange oil. The product was dissolved in 25 mL of ethanol and chilled to −20 °C for 1 h, separating some colorless crystals. The walls of the flask were scraped with a spatula, and with further cooling additional product precipitated. The white solid was collected by filtration, washed with 25 mL of ethanol, and dried in vacuo. Yield: 3.09 g (52.2%). ^{1}H NMR (300 MHz, C_6D_6) δ: 7.57 (m, 4H, Ar*H*), 7.02−7.22 (m, 8H, Ar*H*), 6.79 (m, 1H, Ar*H*), 6.59 (ddd, J = 7.9, 4.7, 1.2 Hz, 1H, Ar*H*), 2.29 (s, 12H, CH_3). ^{13}C{^{1}H} NMR (126 MHz, C_6D_6) δ: 157.4 (d, J_{CP} = 1.3 Hz, *C*═N), 155.2 (d, J_{CP} = 19.3 Hz, Ar), 139.4 (d, J_{CP} = 12.8 Hz, Ar), 134.7 (s, J_{CP} = 20.0 Hz, Ar), 133.5 (d, J_{CP} = 1.6 Hz, Ar), 129.7 (d, J_{CP} = 7.2 Hz, Ar), 129.4 (s, Ar), 128.4 (d, J_{CP} = 6.8 Hz, Ar), 128.2 (s, Ar), 120.6 (d, J_{CP} = 2.4 Hz, Ar), 120.5 (d, J_{CP} = 0.9 Hz, Ar), 39.4 (s, NCH_3). ^{31}P{^{1}H} NMR (121 MHz, C_6D_6) δ: −11.8. Anal. Calcd for $C_{23}H_{26}N_3P$: C, 73.58; H, 6.98; N, 11.19. Found: C, 73.89; H, 7.11; N, 11.12.

Preparation of 6-(Diphenylphosphino)-1,8-diazabicyclo[5.4.0]undec-7-ene (L5). A solution of DBU (3.50 g, 23.0 mmol) in 85 mL of THF was cooled in a dry ice/acetone bath. A pentane solution of *tert*-butyllithium (1.63 M, 15 mL, 24 mmol, 1.05 equiv) was added at a dropwise rate via cannula, giving a yellow solution, from which a yellow solid precipitated during 1 h of stirring. At this time the cold bath was removed, and by allowing the solution to warm to room temperature for 1 h the solid dissolved and most of the color faded. The nearly colorless solution was rechilled in dry ice/acetone, and a solution of Ph_2PCl (5.07 g, 23.0 mmol, 1.00 equiv) dissolved in 20 mL of THF was added, giving an orange solution. After 20 min, the cold bath was removed, and the solution stirred at room temperature overnight. Addition of 2 mL of methanol completely bleached the yellow color, and concentrating in vacuo left a pale yellow residue. The residue was extracted into 50 mL of CH_2Cl_2 and filtered through Celite to remove a white solid. The solvent was removed in vacuo to give a pale sticky solid, which was dissolved in 100 mL of 1:1 CH_2Cl_2/hexane. The solution was concentrated to one-half the original volume, and a white solid collected by filtration. A second crop was isolated from the supernatant. The combined crude products were suspended in 50 mL of boiling EtOH, which was made basic with 6 mL of 25% KOMe/MeOH. The mixture was cooled to −20 °C overnight, filtered, and concentrated by rotary evaporation. The yellow oil was triturated with 50 mL of hexane, releasing a white solid, which was collected by filtration and dried in vacuo. Yield: 3.18 g (41.1%). The spectral properties match those previously reported for this compound, prepared by an alternate route.[23]

Preparation of 2-*tert*-Butyl-6-diphenylphosphino-4-methylphenol (L6). A solution of MOM-protected 2-bromo-6-*tert*-butyl-4-methylphenol (8.50 g, 29.6 mmol) in 100 mL of THF was chilled in a dry ice/acetone bath. A pentane solution of *tert*-butyllithium (40 mL, 65 mmol, 2.2 equiv) was added via cannula, giving a yellow mixture, which was stirred for 45 min while kept cold. After allowing the mixture to briefly warm to room temperature, it was rechilled, and a solution of Ph_2PCl (6.53 g, 29.6 mmol, 1.00 equiv) in 8 mL of THF was added. The color initially lightened, and while stirring overnight at room temperature a deep red color developed. Addition of 2 mL of methanol caused the color to fade to pale orange. The solution was concentrated in vacuo, and the resulting residue dissolved in 100 mL of CH_2Cl_2 and washed with 100 mL of 1 M Na_2HPO_4. The organic layer was dried over $MgSO_4$, filtered, and concentrated to produce a pale orange oil. Trituration with 25 mL of methanol released a white solid, and after cooling to −20 °C for 30 min the MOM-protected product was filtered, washed with methanol, and dried in vacuo. Yield: 8.16 g (70.3%). ^{1}H NMR (300 MHz, $CDCl_3$) δ: 7.22−7.36 (m, 10H, Ar*H*), 7.18 (d, 1H, Ar*H*), 6.47 (ddquart., J = 4.37, 2.10, 0.66 Hz, 1H,

dx.doi.org/10.1021/om400810v | *Organometallics* 2013, 32, 5530−5545

ArH), 5.22 (d, 2H, CH_2), 3.51 (s, 3H, OCH_3), 2.15 (s, 3H, $ArCH_3$), 1.43 (s, 9H, $C(CH_3)_3$). $^{31}P\{^1H\}$ NMR (121 MHz, C_6D_6) δ: −12.8. A sample of the MOM-protected phosphinophenol (5.46 g, 13.9 mmol) was deprotected as previously described.[25] The isolated product **L6** was spectroscopically identical to a previously characterized sample.[26]

Preparation of (L2H)(BF_4). A sample of **L2** (100 mg, 0.313 mmol) was dissolved in 4 mL of Et_2O. With stirring, $HBF_4{\cdot}Et_2O$ (46.1 μL, 0.344 mmol, 1.10 equiv) was added via syringe. A sticky white solid precipitated immediately, and by scraping with a spatula and stirring a white powder was obtained. The supernatant was decanted, and the product dried in vacuo. Yield: 113 mg (89.0%). ^1H NMR (300 MHz, CD_3CN) δ: 9.04 (br, s, 1H, NH), 7.10−7.70 (m, 14H, ArH), 4.44 (d, J = 5.7 Hz, 2H, CH_2), 2.86 (d, J = 5.4 Hz, 6H, CH_3). $^{13}C\{^1H\}$ NMR[45] (126 MHz, CD_3CN) δ: 136.2 (br, s, Ar), 135.2 (s, Ar), 134.9 (br, d, J_{CP} = 18.0 Hz, Ar), 133.0 (d, J_{CP} = 6.2 Hz, Ar), 131.9 (s, Ar), 130.4 (br, s, Ar), 60.2 (br, d, J_{CP} = 17.9 Hz, CH_2), 44.2 (s, CH_3). $^{31}P\{^1H\}$ NMR (121 MHz, CD_3CN) δ: −16.4 (br). HRMS (FAB): m/z calcd for $C_{21}H_{23}NP$ $[M]^+$ 320.1568, found 320.1552.

Preparation of (L3H)(BF_4). Solid **L3** (200 mg, 0.701 mmol) was dissolved in 6 mL of Et_2O. To the stirred solution was added $HBF_4{\cdot}Et_2O$ (98 μL, 0.73 mmol, 1.04 equiv), which caused a sticky white solid to precipitate. After 10 min the supernatant was decanted, and the product was triturated with toluene/Et_2O, which liberated a white solid. After pipetting off the solvents, the product was dried in vacuo. Yield: 189 mg (72.1%). ^1H NMR (300 MHz, CD_3CN) δ: 7.05−7.95 (m, 11H, ArH + NH), 4.00 (br, m, 4H, CH_2), 3.74 (m, 2H, CH_2), 3.58 (br, d, J = 12.6 Hz, 2H, CH_2), 3.18 (br, m, 2H, CH_2). $^{13}C\{^1H\}$ NMR (126 MHz, CD_3CN) δ: 134.2 (br, d, J_{CP} = 20.8 Hz, Ar), 131.3 (br, s, Ar), 130.8 (br, s, Ar), 130.2 (br, d, J_{CP} = 18.0 Hz, Ar), 65.6 (s, CH_2), 59.4 (br, s, CH_2) 55.0 (br, s, CH_2). $^{31}P\{^1H\}$ NMR (121 MHz, CD_3CN) δ: −27.0 (br). HRMS (FAB): m/z calcd for $C_{17}H_{21}ONP$ $[M]^+$ 286.1361, found 286.1351.

Preparation of (L4H)(BF_4). **L4** (200 mg, 0.533 mmol) was dissolved in 1 mL of CH_2Cl_2. Via syringe, $HBF_4{\cdot}Et_2O$ (75 μL, 0.56 mmol, 1.05 equiv) was added, leaving a colorless solution. The solution was stirred at room temperature for 20 min, during which time some white solid formed. Addition of 10 mL of Et_2O further precipitated the product, which was separated from the supernatant by decantation and dried in vacuo. Yield: 240 mg (97.2%). ^1H NMR (300 MHz, CD_3CN) δ: 7.59 (br, s, 1H, NH), 7.20−7.55 (m, 12H, ArH), 7.12 (dd, J = 8.0, 4.7 Hz, 1H, ArH), 7.04 (dd, J = 8.3, 4.1 Hz, 1H, ArH), 2.79 (s, 12H, CH_3). $^{13}C\{^1H\}$ NMR (126 MHz, CD_3CN) δ: 160.2 (s, C═N), 141.9 (d, J_{CP} = 22.8 Hz, Ar), 136.3 (s, Ar), 135.9 (d, J_{CP} = 8.1 Hz, Ar), 134.6 (d, J_{CP} = 20.2 Hz, Ar), 132.2 (s, Ar), 131.8 (br, s, Ar), 130.5 (s, Ar), 130.0 (d, J_{CP} = 7.3 Hz, Ar), 127.9 (s, Ar), 125.1 (s, Ar), 40.8 (s, CH_3). $^{31}P\{^1H\}$ NMR (121 MHz, CD_3CN) δ: −18.9. Anal. Calcd for $C_{23}H_{27}BF_4N_3P$: C, 59.63; H, 5.87; N, 9.07. Found: C, 59.40; H, 5.73; N, 9.04.

Preparation of (L5H)(BF_4). A scintillation vial was charged with **L5** (500 mg, 1.49 mmol) dissolved in 2 mL of CH_2Cl_2. A sample of $HBF_4{\cdot}Et_2O$ (210 μL, 1.56 mmol, 1.05 equiv) was added. The colorless solution was stirred for 10 min, at which point ca. 15 mL of Et_2O was added to precipitate a fluffy, white solid. The supernatant was decanted, and the product washed with Et_2O and dried in vacuo. Yield: 623 mg (98.9%). ^1H NMR (300 MHz, CD_3CN) δ: 7.65−7.75 (m, 2H, ArH), 7.50−7.56 (m, 3H, ArH), 7.36−7.46 (m, 5H, ArH), 7.15 (br, s, 1H, NH), 4.70 (dddd, J_{HH} = 15.2, 11.1, 2.2 Hz, $^2J_{HP}$ = 8.8 Hz, 1H, CH), 3.63 (ddd, J_{HH} = 6.2, 4.1 Hz, J_{HP} = 2.2 Hz, 1H, CH_2), 3.32−3.56 (m, 3H, CH_2), 3.00−3.12 (m, 1H, CH_2), 2.61−2.73 (m, 1H, CH_2), 1.50−2.10 (m, 8H, CH_2). $^{13}C\{^1H\}$ NMR (126 MHz, CD_3CN) δ: 165.3 (d, $^2J_{CP}$ = 7.4 Hz, C═N), 135.2 (d, J_{CP} = 15.5 Hz, Ar), 134.6 (d, J_{CP} = 19.6 Hz, Ar), 134.4 (d, J_{CP} = 18.3 Hz, Ar), 132.1 (d, J_{CP} = 14.5 Hz, Ar), 131.5 (s, Ar), 131.2 (s, Ar), 130.3 (d, J_{CP} = 8.2 Hz, Ar), 129.8 (d, J_{CP} = 7.7 Hz, Ar), 54.7 (d, J_{CP} = 16.0 Hz, CH_2), 50.5 (s, CH_2), 45.2 (d, J_{CP} = 22.3 Hz, CH), 39.2 (s, CH_2), 27.2 (d, J_{CP} = 13.2 Hz, CH_2), 26.8 (s, CH_2), 24.4 (d, J_{CP} = 7.2 Hz, CH_2), 19.4 (s, CH_2). $^{31}P\{^1H\}$ NMR (121 MHz, CD_3CN) δ: −17.5. Anal. Calcd for $C_{21}H_{26}BF_4N_2P$: C, 59.46; H, 6.18; N, 6.60. Found: C, 59.38; H, 6.21; N, 6.58.

Preparation of [Re^I(L1-κ_1-P)$(CO)_5$](BF_4) (1). $Re^I(CO)_5(FBF_3)$ (200 mg, 0.484 mmol) was suspended in 4 mL of CH_2Cl_2. A solution of **L1** (193 mg, 0.484 mmol, 1.00 equiv), dissolved in 2 mL of CH_2Cl_2, was added at a rate of one drop per second, initially giving an orange solution. Over the course of 30 min with continuous stirring, the color faded to yellow. The solvent was removed in vacuo to leave a yellow residue, which was redissolved in 2 mL of CH_2Cl_2. Addition of 2 mL of hexane induced precipitation of a yellow solid, and the mixture was chilled in the freezer (−35 °C) for 3 h. The supernatant was decanted, and the product dried in vacuo. Yield: 306 mg (77.9%). ^1H NMR (300 MHz, CD_2Cl_2) δ: 7.85 (dd, J = 8.8, 2.4 Hz, 1H, ArH), 7.49−7.77 (m, 13H, ArH), 7.38 (dd, J = 7.5, 1.3 Hz, 1H, ArH), 2.56 (s, 6H, CH_3), 2.20 (s, 6H, CH_3). $^{13}C\{^1H\}$ NMR (126 MHz, CD_2Cl_2) δ: 179.4 (br, d, $^2J_{CP}$ = 6.9 Hz, cis CO), 175.2 (br, d, $^2J_{CP}$ = 39.7 Hz, trans CO), 154.7 (d, J_{CP} = 2.5 Hz, Ar), 153.8 (s, Ar), 140.2 (d, J_{CP} = 2.1 Hz, Ar), 133.9 (d, J_{CP} = 54.9 Hz, Ar), 132.6 (d, J_{CP} = 11.2 Hz, Ar), 132.0 (d, J_{CP} = 2.8 Hz, Ar), 129.8 (d, J_{CP} = 11.1 Hz, Ar), 129.4 (d, J_{CP} = 15.2 Hz, Ar), 129.2 (s, Ar), 128.7 (d, J_{CP} = 7.0 Hz, Ar), 127.6 (d, J_{CP} = 60.1 Hz, Ar), 127.5 (d, J_{CP} = 13.5 Hz, Ar), 125.1 (s, Ar), 118.9 (s, Ar), 47.1 (s, CH_3), 44.6 (s, CH_3). $^{31}P\{^1H\}$ NMR (121 MHz, CD_2Cl_2) δ: 1.4. IR (CH_2Cl_2): $\tilde{\nu}_{C\equiv O}$ = 2155 (m), 2094 (w), 2047 (s) cm^{-1}. Anal. Calcd for $C_{31}H_{27}BF_4N_2O_5PRe$: C, 45.88; H, 3.35; N, 3.45. Found: C, 45.64; H, 3.49; N, 3.36.

Preparation of [Re^I(L2-κ_1-P)$(CO)_5$](OTf) (2). $Re^I(CO)_5(OTf)$ (100 mg, 0.210 mmol) and **L2** (67 mg, 0.21 mmol, 1.0 equiv) were dissolved in 5 mL of CH_2Cl_2 in a 20 mL flask sealed with a Teflon plug. The solution was stirred for 1 week at room temperature, at which time the crude $^{31}P\{^1H\}$ NMR spectrum indicated ca. 90% completion. The solution was filtered to remove a small amount of a brown impurity and then concentrated in vacuo. The residue was redissolved in 2 mL of THF, and by adding 8 mL of Et_2O a white solid precipitated, which was decanted and dried in vacuo. Yield: 116 mg of **2**·THF (69.5%). ^1H NMR (300 MHz, CD_2Cl_2) δ: 7.50−7.75 (m, 14H, ArH), 3.68 (m, THF), 2.98 (s, 2H, CH_2), 1.82 (m, THF), 1.68 (s, 6H, CH_3). $^{13}C\{^1H\}$ NMR (126 MHz, CD_2Cl_2) δ: 179.1 (br, d, $^2J_{CP}$ = 6.6 Hz, cis CO), 175.3 (br, d, $^2J_{CP}$ = 42.1 Hz, trans CO), 142.9 (s, Ar), 135.0 (d, J_{CP} = 14.6 Hz, Ar), 133.7 (d, J_{CP} = 8.6 Hz, Ar), 133.1 (d, J_{CP} = 11.6 Hz, Ar), 132.8 (s, Ar), 132.6 (d, J_{CP} = 2.8 Hz, Ar), 132.4 (s, Ar), 132.0 (s, Ar), 130.2 (d, J_{CP} = 11.2 Hz, Ar), 128.8 (d, J_{CP} = 12. Hz, Ar), 121.4 (quart., $^1J_{CF}$ = 322.6 Hz, CF_3), 68.1 (s, THF), 63.1 (s, CH_2), 44.8 (s, CH_3), 25.9 (s, THF). $^{31}P\{^1H\}$ NMR (121 MHz, CD_2Cl_2) δ: 5.3. IR (CH_2Cl_2): $\tilde{\nu}_{C\equiv O}$ = 2156 (m), 2095 (w), 2048 (s) cm^{-1}. Anal. Calcd for $C_{31}H_{30}F_3NO_9PReS$ (**2**·THF): C, 42.96; H, 3.49; N, 1.62. Found: C, 42.66; H, 3.46; N, 1.49.

Preparation of [Re^I(L3-κ_1-P)$(CO)_5$](BF_4) (3). A scintillation vial was charged with $Re^I(CO)_5(FBF_3)$ (200 mg, 0.484 mmol) suspended in 2 mL of CH_2Cl_2. A solution of **L3** (138 mg, 0.484 mmol, 1.00 equiv) in 3 mL of CH_2Cl_2 was added. A colorless solution resulted, which was stirred for 30 min at room temperature. Addition of 15 mL of Et_2O separated a white residue, from which the supernatant was decanted. The residue was dissolved in 2 mL of THF, and with addition of 6 mL of Et_2O a sticky solid separated. The solid was suspended in 4 mL of Et_2O and stirred overnight, producing a freely flowing white powder, which was dried in vacuo. Yield: 277 mg (82.0%). ^1H NMR (300 MHz, CD_2Cl_2) δ: 7.30−7.90 (m, 10H, ArH), 3.84 (d, $^2J_{HP}$ = 3.9 Hz, 4H, CH_2), 3.54 (m, 4H, CH_2), 2.35 (m, 4H, CH_2). $^{13}C\{^1H\}$ NMR (126 MHz, CD_2Cl_2) δ: 178.6 (br, s, cis CO), 175.7 (br, s, trans CO), 133.1 (d, J_{CP} = 2.5 Hz, Ar), 132.4 (d, J_{CP} = 10.1 Hz, Ar), 130.9 (d, J_{CP} = 50.3 Hz, Ar), 130.4 (d, J_{CP} = 10.4 Hz, Ar), 66.5 (s, CH_2), 60.3 (d, J_{CP} = 47.5 Hz, CH_2), 55.9 (d, J_{CP} = 7.8 Hz, CH_2). $^{31}P\{^1H\}$ NMR (121 MHz, CD_2Cl_2) δ: 3.8 (br). IR (CH_2Cl_2): $\tilde{\nu}_{C\equiv O}$ = 2157 (m), 2099 (w), 2047 (s) cm^{-1}. Anal. Calcd for $C_{22}H_{20}BF_4NO_6PRe$: C, 37.84; H, 2.89; N, 2.01. Found: C, 38.06; H, 3.01; N, 1.96.

Preparation of [Re^I(L4-κ_1-P)$(CO)_5$](BF_4) (4). To a suspension of $Re^I(CO)_5(FBF_3)$ (200 mg, 0.484 mmol) in 2 mL of CH_2Cl_2 was added a solution of **L4** (182 mg, 0.485 mmol, 1.00 equiv) in 3 mL of CH_2Cl_2. The solid was drawn into solution, with a pale yellow color resulting. After stirring for 30 min at room temperature, 15 mL of Et_2O was gradually added, which separated an eggshell-colored solid. The supernatant was decanted, and the product washed with 4 mL of Et_2O and dried in vacuo. Yield: 356 mg (93.2%). ^1H NMR (300 MHz,

dx.doi.org/10.1021/om400810v | Organometallics 2013, 32, 5530−5545

CD_3CN) δ: 7.35−7.65 (m, 12H, ArH), 6.95 (dddd, J = 8.1, 7.1, 2.1, 1.1 Hz, 1H, ArH), 6.41 (ddd, J = 8.2, 5.8, 1.2 Hz, 1H, ArH), 2.37 (s, 12H, CH_3). $^{13}C\{^1H\}$ NMR (126 MHz, CD_3CN) δ: 181.2 (br, s, cis CO), 178.2 (br, d, $^2J_{CP}$ = 39.1 Hz, trans CO), 163.6 (s, C═N), 156.8 (d, J_{CP} = 8.6 Hz, Ar), 134.4 (s, Ar), 134.3 (d, J_{CP} = 10.7 Hz, Ar), 133.7 (d, J_{CP} = 6.0 Hz, Ar), 132.7 (d, J_{CP} = 2.5 Hz, Ar), 132.6 (d, J_{CP} = 53.0 Hz, Ar), 130.1 (d, J_{CP} = 10.7 Hz, Ar), 122.9 (d, J_{CP} = 6.9 Hz, Ar), 119.8 (d, J_{CP} = 9.8 Hz, Ar), 115.9 (d, J_{CP} = 57.8 Hz, Ar), 39.7 (s, CH_3). $^{31}P\{^1H\}$ NMR (121 MHz, CD_3CN) δ: −7.2. IR (CH_2Cl_2): $\tilde{\nu}_{C\equiv O}$ = 2150 (m), 2088 (w), 2047 (s) cm^{-1}. Anal. Calcd for $C_{28}H_{26}BF_4N_3O_5PRe$: C, 42.65; H, 3.32; N, 5.33. Found: C, 42.62; H, 3.41; N, 5.20.

In Situ Preparation of [Re^I(L5-κ_1-P)(CO)$_5$](BF$_4$) (5). Because of its instability with regard to forming the κ_2-P,N complex (**7**) (see below), complex **5** was not isolated. We identified and characterized it in solution either from the crude reaction between $Re^I(CO)_5(FBF_3)$ and 1 equivalent of **L5** (ca. 80% yield at early time points) or by deprotonation of complex **12** (see below) with triethylamine (quantitative yield). ^1H NMR (300 MHz, CD_3CN) δ: 7.65−7.80 (m, 2H, ArH), 7.35−7.60 (m, 8H, ArH), 4.10 (app. t, $^2J_{HP}$ = J_{HH} = 10.0 Hz, 1H, CH) 3.84 (dd, J = 15.3, 10.4 Hz, 1H, CH_2), 2.95−3.32 (m, 5H, CH_2), 1.35−2.07 (m, 8H, CH_2). $^{31}P\{^1H\}$ NMR (121 MHz, CD_3CN) δ: 3.6 (br). IR (CH_2Cl_2) $\tilde{\nu}_{C\equiv O}$ = 2151 (m), 2091 (w), 2041(s) cm^{-1}.

Preparation of [Re^I(L6-κ_1-P)(CO)$_5$](BF$_4$) (6). Solid $Re^I(CO)_5(FBF_3)$ (200 mg, 0.484 mmol) was suspended in 4 mL of CH_2Cl_2. A solution of **L6** (169 mg, 0.485 mmol, 1.00 equiv) dissolved in 4 mL of CH_2Cl_2 was added, producing a colorless solution. After stirring for 90 min, the solvent was removed in vacuo. The colorless residue was redissolved in 2 mL of CH_2Cl_2, and with stirring 6 mL of Et_2O was added. The white solid that precipitated was separated by decanting the mother liquor and then washed with Et_2O and dried in vacuo. Yield: 347 mg of **6**·CH_2Cl_2 (84.6%). ^1H NMR (300 MHz, CD_3CN) δ: 7.51−7.65 (m, 6H, ArH), 7.35−7.50 (m, 5H, ArH), 6.82 (d, J = 12.0 Hz, 1H, ArH), 6.58 (s, 1H, OH), 5.45 (s, CH_2Cl_2), 2.22 (s, 3H, ArCH_3), 1.37 (s, 9H, C(CH_3)$_3$). $^{13}C\{^1H\}$ NMR (126 MHz, CD_3CN) δ: 180.8 (d, $^2J_{CP}$ = 6.2 Hz, cis CO), 177.6 (br, d, $^2J_{CP}$ = 42.1 Hz, trans CO), 154.0 (d, $^2J_{CP}$ = 5.3 Hz, Ar), 139.6 (d, J_{CP} = 5.3 Hz, Ar), 133.9 (d, J_{CP} = 11.3 Hz, Ar), 133.9 (s, Ar), 133.0 (d, J_{CP} = 2.5 Hz, Ar), 132.6 (d, J_{CP} = 10.2 Hz, Ar), 131.9 (d, J_{CP} = 5.4 Hz, Ar) 131.4 (d, J_{CP} = 54.3 Hz, Ar), 130.5 (d, J_{CP} = 11.0 Hz, Ar), 119.0 (d, J_{CP} = 56.1 Hz, Ar), 34.9 (s, C(CH$_3$)$_3$), 30.4 (s, C(CH_3)$_3$), 21.0 (s, ArCH_3). $^{31}P\{^1H\}$ NMR (121 MHz, CD_2Cl_2) δ: −4.6. IR (CH_2Cl_2): $\tilde{\nu}_{C\equiv O}$ = 2157 (m), 2102 (w), 2048 (s) cm^{-1}. Anal. Calcd for $C_{29}H_{27}BCl_2F_4O_6PRe$ (**6**·CH_2Cl_2): C, 41.15; H, 3.22; N, 0.00. Found: C, 40.99; H, 3.16; N, 0.

Preparation of [Re^I(L5-κ_2-P,N)(CO)$_4$](BF$_4$) (7). A sample of crude **5** (357 mg), prepared by reaction of $Re^I(CO)_5(FBF_3)$ with **L5**, was dissolved in 6 mL of CH_2Cl_2 and held at room temperature for ca. 60 h. The solution was concentrated in vacuo to produce a colorless residue, which was redissolved in 2 mL of CH_2Cl_2. Addition of 8 mL of Et_2O separated a white solid; the supernatant was removed and the product dried in vacuo. Yield: 325 mg (94.5%). ^1H NMR (300 MHz, CD_2Cl_2) δ: 7.45−7.85 (m, 8H, ArH), 7.22−7.32 (m, 2H, ArH), 4.49 (ddd, $^2J_{HP}$ = 14.3 Hz, J_{HH} = 9.8, 2.4 Hz, 1H, CH), 4.24 (dd, J_{HH} = 15.8, 10.4 Hz, 1H, CH_2), 3.36−3.76 (m, 5H, CH_2), 1.35−2.15 (m, 8H, CH_2). $^{13}C\{^1H\}$ NMR (126 MHz, CD_2Cl_2) δ: 186.6 (d, $^2J_{CP}$ = 6.7 Hz, cis CO), 185.3 (d, $^2J_{CP}$ = 46.9 Hz, trans CO), 185.1 (d, $^2J_{CP}$ = 8.3 Hz, cis CO), 183.6 (d, $^2J_{CP}$ = 8.4 Hz, cis CO), 171.2 (d, $^2J_{CP}$ = 12.3 Hz, C═N), 135.3 (d, J_{CP} = 12.7 Hz, Ar), 134.8 (s, Ar), 133.9 (d, J_{CP} = 2.6 Hz, Ar), 132.1 (d, J_{CP} = 2.4 Hz, Ar), 130.6 (d, J_{CP} = 11.6 Hz, Ar), 130.2 (d, J_{CP} = 10.4 Hz, Ar) 130.0 (d, J_{CP} = 10.1 Hz, Ar), 125.6 (d, J_{CP} = 56.1 Hz, Ar), 58.1 (d, J_{CP} = 4.7 Hz, CH_2), 56.1 (s, CH_2), 49.2 (d, J_{CP} = 34.6 Hz, CH), 49.1 (s, CH_2), 28.0 (d, J_{CP} = 9.4 Hz, CH_2), 27.1 (s, CH_2), 26.8 (s, CH_2), 23.1 (s, CH_2). $^{31}P\{^1H\}$ NMR (121 MHz, CD_2Cl_2) δ: 23.4. IR (CH_2Cl_2): $\tilde{\nu}_{C\equiv O}$ = 2109 (m), 2020 (s), 2006 (s), 1968 (s) cm^{-1}. Anal. Calcd for $C_{25}H_{25}BF_4N_2O_4PRe$: C, 41.62; H, 3.49; N, 3.88. Found: C, 40.97; H, 3.56; N, 3.66.

Preparation of [Re^I(L1H-κ_1-P)(CO)$_5$](BF$_4$)$_2$ (8). A scintillation vial was charged with **1** (100 mg, 0.123 mmol) dissolved in 4 mL of CH_2Cl_2. To the yellow solution was added HBF_4·Et_2O (18 μL, 0.13 mmol, 1.1 equiv), which immediately resulted in the formation of a white solid. The mixture was stirred for 10 min and then allowed to settle. The supernatant was decanted, and the product washed with 2 mL of CH_2Cl_2 and 2 × 2 mL of Et_2O before drying in vacuo. Yield: 101 mg (91.0%). ^1H NMR (300 MHz, CD_3CN) δ: 17.08 (br, s, NH), 8.24 (dd, J = 3.6, 1.3 Hz, 1H, ArH), 8.21 (dd, J = 2.9, 1.3 Hz, 1H, ArH), 8.08 (dd, J = 7.8, 1.3 Hz, 1H, ArH), 7.87−8.02 (m, 2H, ArH), 7.59−7.74 (m, 10H, ArH), 3.29 (d, J = 4.2 Hz, 6H, CH_3), 2.50 (d, J = 0.6 Hz, 6H, CH_3). $^{13}C\{^1H\}$ NMR (126 MHz, CD_3CN) δ: 180.2 (d, $^2J_{CP}$ = 8.2 Hz, cis CO), 176.2 (d, $^2J_{CP}$ = 42.8 Hz, trans CO), 149.3 (s, Ar), 143.1 (s, Ar), 138.4 (s, Ar), 135.8 (d, J_{CP} = 11.8 Hz, Ar), 134.7 (d, J_{CP} = 18.1 Hz, Ar), 134.2 (d, J_{CP} = 2.6 Hz, Ar), 133.2 (d, J_{CP} = 50.9 Hz, Ar) 132.5 (d, J_{CP} = 37.9 Hz, Ar), 132.0 (s, Ar), 130.9 (d, J_{CP} = 11.2 Hz, Ar), 130.5 (s, Ar), 130.0 (d, J_{CP} = 13.7 Hz, Ar), 124.1 (s, Ar), 123.4 (d, J_{CP} = 8.2 Hz, Ar), 48.2 (s, CH_3), 44.8 (s, CH_3). $^{31}P\{^1H\}$ NMR (121 MHz, CD_2Cl_2) δ: 14.9. IR (CH_3CN): $\tilde{\nu}_{C\equiv O}$ = 2160 (m), 2054 (s) cm^{-1}. Anal. Calcd for $C_{31}H_{28}B_2F_8N_2O_5PRe$: C, 41.40; H, 3.14; N, 3.11. Found: C, 40.89; H, 3.17; N, 2.95.

Preparation of [Re^I(L2H-κ_1-P)(CO)$_5$](BF$_4$)(OTf) (9). Solid **2**·THF (56 mg, 0.065 mmol) was dissolved in 2 mL of CH_2Cl_2. Via syringe, HBF_4·Et_2O (10 μL, 0.075 mmol, 1.1 equiv) was added with stirring, causing a white solid to precipitate. After stirring briefly, the mixture was diluted with 4 mL of Et_2O and decanted, and the product was dried in vacuo. Yield: 56 mg (98%). ^1H NMR (300 MHz, CD_3CN) δ: 8.24 (m, 1H, ArH), 7.95 (m, 2H, ArH), 7.63−7.76 (m, 11H, ArH), 7.48 (br, s, 1H, NH), 3.68 (d, J = 6.3 Hz, 2H, CH_2), 2.08 (d, J = 5.1 Hz, 6H, CH_3). $^{13}C\{^1H\}$ NMR (126 MHz, CD_3CN) δ: 180.0 (d, $^2J_{CP}$ = 8.3 Hz, cis CO), 176.7 (d, $^2J_{CP}$ = 42.2 Hz, trans CO), 140.7 (d, J_{CP} = 21.7 Hz, Ar), 135.8 (d, J_{cp} = 2.6 Hz, Ar), 134.7 (s, Ar), 133.8 (d, J_{CP} = 2.0 Hz, Ar), 132.6 (d, J_{CP} = 11.0 Hz, Ar), 132.1 (d, J_{CP} = 6.3 Hz, Ar), 131.8 (d, J_{CP} = 34.8 Hz, Ar), 131.5 (s, Ar), 131.4 (s, Ar), 128.0 (d, J_{CP} = 49.3 Hz, Ar), 121.9 (quart., $^1J_{CF}$ = 320.1 Hz, CF_3), 59.0 (d, J_{CP} = 5.0 Hz, CH_2), 43.7 (s, CH_3). $^{31}P\{^1H\}$ NMR (121 MHz, CD_3CN) δ: 2.6. IR (CH_3CN): $\tilde{\nu}_{C\equiv O}$ = 2160 (m), 2053 (s) cm^{-1}. Anal. Calcd for $C_{27}H_{23}BF_7NO_8PReS$: C, 36.75; H, 2.63; N, 1.59. Found: C, 36.76; H, 2.74; N, 1.56.

Preparation of [Re^I(L3H-κ_1-P)(CO)$_5$](BF$_4$)$_2$ (10). Complex **3** (100 mg, 0.143 mmol) was dissolved in 2 mL of CH_2Cl_2. HBF_4·Et_2O (20 μL, 0.15 mmol, 1.05 equiv) was added via syringe, which separated a colorless residue from the solution. After 10 min, the mixture was diluted with 8 mL of Et_2O, and by scraping with a spatula a white solid was produced. The supernatant was decanted, and the product dried in vacuo. Yield: 99 mg (88%). ^1H NMR (300 MHz, CD_3CN) δ: 7.55−8.00 (m, 10H, ArH), 7.23 (br, s, 1H, NH), 4.63 (d, J = 5.1 Hz, 2H, CH_2), 3.83 (d, J = 13.5 Hz, 2H, CH_2), 3.58 (t, J = 12.0 Hz, 2H, CH_2), 3.30 (m, 2H, CH_2), 3.09 (d, J = 12.6 Hz, 2H, CH_2). $^{13}C\{^1H\}$ NMR (126 MHz, CD_3CN) δ: 178.7 (d, $^2J_{CP}$ = 6.3 Hz, cis CO), 176.2 (d, $^2J_{CP}$ = 42.5 Hz, trans CO), 135.0 (s, Ar), 133.5 (d, J_{cp} = 11.5 Hz, Ar), 131.7 (d, J_{CP} = 11.6 Hz, Ar), 125.2 (d, J_{CP} = 52.5 Hz, Ar), 63.8 (s, CH_2), 56.9 (s, CH_2), 56.8 (s, CH_2, overlap with previous peak). $^{31}P\{^1H\}$ NMR (121 MHz, CD_3CN) δ: −5.4. IR (CH_3CN): $\tilde{\nu}_{C\equiv O}$ = 2163 (m), 2157 (w), 2056 (s) cm^{-1}. Anal. Calcd for $C_{22}H_{21}B_2F_8NO_6PRe$: C, 33.61; H, 2.69; N, 1.78. Found: C, 33.70; H, 2.79; N, 1.78.

Preparation of [Re^I(L4H-κ_1-P)(CO)$_5$](BF$_4$)$_2$ (11). A scintillation vial was charged with **4** (100 mg, 0.127 mmol) dissolved in 2 mL of CH_2Cl_2. To this solution was added HBF_4·Et_2O (18 μL, 0.13 mmol, 1.05 equiv). A white solid immediately formed, and after 10 min 8 mL of Et_2O was added to the mixture. After allowing the product to settle, the supernatant was decanted, and the remaining white powder was washed with Et_2O and dried in vacuo. Yield: 110 mg of **11**·CH_2Cl_2 (90.3%). ^1H NMR (300 MHz, CD_3CN) δ: 8.15 (ddd, J = 17.9, 7.8, 1.6 Hz, 1H, ArH), 7.64−7.89 (m, 12H, ArH), 6.94 (dd, J = 8.1, 4.1 Hz, 1H, ArH), 5.73 (s, 1H, NH), 5.45 (s, CH_2Cl_2), 2.40 (br, s, 12H, CH_3). $^{13}C\{^1H\}$ NMR (126 MHz, CD_3CN) δ: 179.8 (d, $^2J_{CP}$ = 8.3 Hz, cis CO), 176.6 (d, $^2J_{CP}$ = 42.5 Hz, trans CO), 157.4 (s, C═N), 140.3 (d, J_{cp} = 20.4 Hz, Ar), 140.0 (d, J_{CP} = 2.3 Hz, Ar), 137.1 (d, J_{CP} = 2.4 Hz, Ar), 134.1 (d, J_{CP} = 2.6 Hz, Ar), 132.6 (d, J_{CP} = 11.2 Hz, Ar), 131.6 (d, J_{CP} = 10.9 Hz, Ar), 129.2 (d, J_{CP} = 50.6 Hz, Ar), 127.7 (d, J_{CP} = 14.0 Hz, Ar), 123.9 (s, Ar), 117.8 (d, J_{CP} = 48.6 Hz, Ar), 55.3 (s, CH_2Cl_2),

dx.doi.org/10.1021/om400810v | Organometallics 2013, 32, 5530−5545

40.5 (br, s, CH_3). $^{31}P\{^1H\}$ NMR (121 MHz, CD_3CN) δ: 1.2. IR (CH_3CN): $\tilde{\nu}_{C\equiv O}$ = 2160 (m), 2053 (s) cm^{-1}. Anal. Calcd for $C_{29}H_{29}B_2Cl_2F_8N_3O_5PRe$ (**11**·CH_2Cl_2): C, 36.24; H, 3.04; N, 4.37. Found: C, 36.39, H, 3.13, N, 4.25.

Preparation of [Re^I(L5H-κ_1-P)(CO)$_5$](BF$_4$)$_2$ (12). A mixture of $Re^I(CO)_5(BF_4)$ (200 mg, 0.484 mmol) and (**L5H**)(**BF$_4$**) (205 mg, 0.483 mmol, 1.00 equiv) in 25 mL of CH_2Cl_2 was sealed in a 75 mL flask with a Teflon plug. The mixture was heated to 50 °C for 4 h, initially giving a colorless solution from which a white solid deposited. The volatiles were removed in vacuo, and the solid was dissolved in MeCN and transferred to a scintillation vial. The solvent was removed under vacuum, and the residue twice triturated with CH_2Cl_2/Et_2O to produce a white powder, which was dried in vacuo. Yield: 346 mg (85.4%). ^1H NMR (300 MHz, CD_3CN) δ: 7.62−7.84 (m, 10H, Ar*H*), 6.71 (br, s, 1H, N*H*), 4.40 (ddd, $^2J_{HP}$ = 9.5 Hz, J_{HH} = 9.4, 6.0 Hz, 1H, C*H*), 3.02−3.47 (m, 5H, CH_2), 2.46 (m, 1H, CH_2), 1.37−2.10 (m, 8H, CH_2). $^{13}C\{^1H\}$ NMR (126 MHz, CD_3CN) δ: 179.2 (d, $^2J_{CP}$ = 8.2 Hz, cis CO), 176.0 (d, $^2J_{CP}$ = 43.2 Hz, trans CO), 151.4 (br, s, C═N), 134.8 (br, d, J_{cp} = 76.9 Hz, Ar), 133.4 (br, s, Ar), 131.8 (d, J_{CP} = 10.5 Hz, Ar), 131.3 (d, J_{CP} = 10.8 Hz, Ar), 51.8 (br, s, CH_2), 50.5 (s, CH_2), 45.5 (d, J_{CP} = 18.7 Hz, CH), 40.5 (s, CH_2), 27.1 (s, CH_2), 24.2 (s, CH_2, overlapped with another broad signal), 19.0 (s, CH_2). $^{31}P\{^1H\}$ NMR (121 MHz, CD_3CN) δ: 9.0 (br). IR (CH_3CN): $\tilde{\nu}_{C\equiv O}$ = 2161 (m), 2054 (s) cm^{-1}. Anal. Calcd for $C_{26}H_{26}B_2F_8N_2O_5PRe$: C, 37.30; H, 3.13; N, 3.35. Found: C, 37.63; H, 3.39; N, 3.24.

In Situ Preparation of Re^I(L6$^-$-κ_1-P)(CO)$_5$ (13). Complex **6** can be deprotonated with a variety of suitably strong bases. In a typical experiment, complex **6**·CH_2Cl_2 (25 mg, 0.030 mmol) in 0.7 mL of CD_3CN was treated with 1.1 equivalents of DBU, delivered from a stock solution. The initially colorless solution turned pale yellow. The NMR spectra showed, in addition to peaks for protonated DBU, quantitative formation of **13**, which has a half-life of ca. 3 h at room temperature (see below for details of the decomposition). ^1H NMR (300 MHz, CD_3CN) δ: 7.50−7.66 (m, 7H, Ar*H*), 7.36−7.45 (m, 4H, Ar*H*), 6.06 (ddd, J = 11.1, 2.1, 0.8 Hz, 1H, Ar*H*), 2.08 (s, 3H, ArCH_3), 1.42 (s, 9H, C(CH_3)$_3$). $^{31}P\{^1H\}$ NMR (121 MHz, CD_3CN) δ: 1.8. IR (CH_3CN): $\tilde{\nu}_{C\equiv O}$ = 2100 (m), 2074 (m), 1996 (s) cm^{-1}.

Conversion of 13 to κ_2-P,O Products. Within 15 h at room temperature in acetonitrile, complex **13** decomposes in two stages; initially two products are evident before gradual conversion to a single species. At early time points, the intermediate present is Re^I(**L6**$^-$-κ_2-P,O)(CO)$_4$ (**14**), which converts slowly to *fac*-Re^I(**L6**$^-$-κ_2-P,O)-(NCMe)(CO)$_3$ (**15**). At 80 °C, a good yield of **15**, starting from **13**, occurs within 24 h. Complex **14** is prepared as the major product by heating **13** to 50 °C in CH_2Cl_2 solution. Complexes **14** and **15** can be separated from protonated DBU by extracting into Et_2O and filtering to remove the (DBUH)(BF_4). The following spectral characteristics are noted for the two products. **14**: ^1H NMR (300 MHz, CD_2Cl_2) δ: 7.36−7.64 (m, 10H, Ar*H*), 7.03 (d, J = 2.2 Hz, 1H, Ar*H*), 6.92 (ddd, J = 8.7, 2.2, 1.0 Hz, 1H, Ar*H*), 2.21 (s, 3H, ArCH_3), 1.35 (s, 9H, C(CH_3)$_3$). $^{13}C\{^1H\}$ NMR (126 MHz, CD_2Cl_2) δ: 190.0 (br, s, cis CO), 188.0 (d, $^2J_{CP}$ = 50.1 Hz, trans CO), 186.8 (d, $^2J_{CP}$ = 9.1 Hz, cis CO), 177.2 (d, J_{CP} = 23.7 Hz, ArCO), 142.0 (d, J_{cp} = 7.6 Hz, Ar), 134.2 (d, J_{CP} = 53.5 Hz, Ar), 132.6 (d, J_{CP} = 11.4 Hz, Ar), 131.7 (d, J_{CP} = 2.0 Hz, Ar), 131.1 (d, J_{CP} = 2.6 Hz, Ar), 130.3 (s, Ar), 129.3 (d, J_{CP} = 10.8 Hz, Ar), 124.2 (d, J_{CP} = 8.3 Hz, Ar), 112.7 (d, J_{CP} = 57.9 Hz, Ar), 35.4 (s, C(CH_3)$_3$), 29.4 (s, C(CH_3)$_3$), 20.6 (s, ArCH$_3$). $^{31}P\{^1H\}$ NMR (121 MHz, CD_2Cl_2) δ: 25.1. IR (CH_2Cl_2): $\tilde{\nu}_{C\equiv O}$ = 2101 (m), 2001 (s), 1933 (m), 1874 (w) cm^{-1}. **15**: ^1H NMR (300 MHz, C_6D_6) δ: 7.79 (m, 2H, Ar*H*), 7.68 (m, 2H, Ar*H*), 7.27 (d, J = 2.2 Hz, 1H, Ar*H*), 7.09 (ddd, J = 8.3, 2.3, 0.8 Hz, 1H, Ar*H*), 6.87−7.04 (m, 6H, Ar*H*), 2.17 (s, 3H, ArCH_3), 1.73 (s, 9H, C(CH_3)$_3$), 0.00 (d, $^5J_{HP}$ = 1.4 Hz, NCCH_3). $^{13}C\{^1H\}$ NMR (126 MHz, CD_2Cl_2) δ: 196.4 (d, J_{CP} = 6.6 Hz, cis CO), 194.4 (d, $^2J_{CP}$ = 7.8 Hz, cis CO), 193.2 (d, $^2J_{CP}$ = 65.4 Hz, trans CO), 176.9 (d, J_{CP} = 25.0 Hz, ArCO), 141.2 (d, J_{cp} = 7.7 Hz, Ar), 133.5 (d, J_{CP} = 10.8 Hz, Ar), 133.2 (d, J_{CP} = 11.5 Hz, Ar), 131.4 (d, J_{CP} = 1.9 Hz, Ar), 130.6 (d, J_{CP} = 2.3 Hz, Ar), 130.5 (s, Ar), 130.3 (d, J_{CP} = 2.4 Hz, Ar), 129.0 (d, J_{CP} = 5.7 Hz, Ar), 128.9 (d, J_{CP} = 6.8 Hz, Ar), 123.4 (d, J_{CP} = 7.6 Hz, Ar), 119.9 (s, NCCH$_3$), 112.1 (d, J_{CP} = 54.8 Hz, Ar), 35.4 (d, J_{CP} = 2.1 Hz, C(CH_3)$_3$), 29.4 (s, C(CH_3)$_3$), 20.7 (s, ArCH$_3$), 2.6 (s, NCCH$_3$). $^{31}P\{^1H\}$ NMR (121 MHz, C_6D_6) δ: 33.9. IR (CH_2Cl_2): $\tilde{\nu}_{C\equiv N}$ = 2306 (w); $\tilde{\nu}_{C\equiv O}$ = 2024 (s), 1930 (s), 1892 (s) cm^{-1}. When dissolved in CD_3CN, the ^1H NMR spectrum of **15** shows one equivalent of free CH_3CN in addition to the peaks attributed to the phosphine ligand.

Preparation of Re^I Formyl Complexes from W−H. The general procedure is described here. Attempts to isolate rhenium formyl complexes were not successful, owing to the difficulty of separating the products from the tungsten-containing product, as well as hastened decarbonylation when the formyl complexes are subjected to vacuum to remove solvent. Therefore the formyl complexes were exclusively studied in solution by spectroscopic means. To prepare the formyl complexes **16**−**20**, rhenium complexes **1**−**5** (25 mg) and 1.1 equivalents of **W−H** were dissolved each in ca. 0.35 mL of CD_3CN. Both solutions were frozen in the glovebox cold well, and upon thawing, the solution of **W−H** was added dropwise. The solution was transferred to an NMR tube, where it was allowed to warm to room temperature. Later experiments showed that the rhenium complex and **W−H** could be mixed at room temperature with no effect on the observed yield of the formyl product. Specific details and spectral features pertaining to the formyl complexes prepared in this way are given below. In all cases, the tungsten-containing product was identified as $W^0(P(OMe)_3)(NCMe)(CO)_4$ (**W^0**), consistent with the observed NMR spectra and possessing a nearly identical IR spectrum to the closely related P(O^{i}Pr)$_3$-substituted analogue.[35] In addition, NMR features for the bis(triphenylphosphine)iminium (PPN^+) cation were present and likewise match previously reported data.[46] The spectroscopic data for these two byproducts, which are present in all samples of rhenium formyl complexes, are as follows. **W^0**: ^1H NMR (300 MHz, CD_3CN) δ: 3.64 (d, $^3J_{HP}$ = 11.4 Hz, 9H, CH_3). $^{13}C\{^1H\}$ NMR (126 MHz, CD_3CN): 205.9 (d, $^2J_{CP}$ = 50.6 Hz, trans CO), 205.4 (d, $^2J_{CP}$ = 8.2 Hz, cis CO), 201.4 ($^2J_{CP}$ = 11.0 Hz, $^1J_{CW}$ = 129.0 Hz, cis CO), 52.4 (s, CH_3). $^{31}P\{^1H\}$ NMR (121 MHz, CD_3CN) δ: 146.8 ($^1J_{PW}$ = 384 Hz). IR (CH_3CN): $\tilde{\nu}_{C\equiv O}$ = 2026 (w), 1905 (s), 1862 (m) cm^{-1}. PPN^+: ^1H NMR (300 MHz, CD_3CN) δ: 7.43−7.70 (m, 30H, Ar*H*). $^{13}C\{^1H\}$ NMR (126 MHz, CD_3CN): 134.6 (s, Ar), 133.2 (m, Ar), 130.4 (m, Ar), 128.2 (dd, J_{CP} = 108, 2.1 Hz, Ar). $^{31}P\{^1H\}$ NMR (121 MHz, CD_3CN) δ: 21.9.

Preparation of *cis*-Re^I(L1-κ_1-P)(CO)$_4$(CHO) (16). Following the procedure described above, complex **16** was prepared by treating **1** (25 mg, 0.031 mmol) with **W−H** (33 mg, 0.034 mmol, 1.1 equiv). Formyl **16** formed in ca. 90% yield, as judged by integration of the ^1H NMR spectrum. ^1H NMR (300 MHz, CD_3CN) δ: 14.91 (s, 1H, C*H*O), 7.25−7.83 (m, 15H, Ar*H*, overlapped with PPN^+), 2.57 (s, 6H, CH_3), 2.28 (s, 6H, CH_3). $^{13}C\{^1H\}$ NMR (126 MHz, CD_3CN) δ: 259.4 (d, $^2J_{CP}$ = 9.1 Hz, CHO), 191.1 (d, $^2J_{CP}$ = 7.4 Hz, cis CO), 190.7 (d, $^2J_{CP}$ = 9.3 Hz, cis CO), 188.1 (d, $^2J_{CP}$ = 42.6 Hz, trans CO), 154.5 (s, Ar), 153.4 (s, Ar), 139.9 (s, Ar), 137.0 (d, J_{CP} = 48.8 Hz, Ar), 135.1 (d, J_{CP} = 11.9 Hz, Ar), 134.4 (d, J_{CP} = 11.9 Hz, Ar) 131.2 (d, J_{CP} = 2.5 Hz, Ar), 131.1 (d, J_{CP} = 15.2 Hz, Ar), 129.2 (d, J_{CP} = 10.5 Hz, Ar), 128.9 (d, J_{CP} = 10.5 Hz, Ar), 128.8 (s, Ar), 125.4 (d, J_{CP} = 12.1 Hz, Ar), 124.6 (s, Ar), 117.8 (s, Ar), 47.0 (s, CH_3), 44.4 (s, CH_3). $^{31}P\{^1H\}$ NMR (121 MHz, CD_3CN) δ: 15.8. IR (CH_3CN): $\tilde{\nu}_{C\equiv O}$ = 2089 (m), 1994 (sh), 1983 (s), 1959 (s) cm^{-1}; $\tilde{\nu}_{C=O}$ = 1590 (m) cm^{-1}.

Preparation of *cis*-Re^I(L2-κ_1-P)(CO)$_4$(CHO) (17). Following the general procedure, complex **17** was prepared from **2**·THF (25 mg, 0.029 mmol) and **W−H** (33 mg, 0.034 mmol, 1.2 equiv) in ca. 95% yield as judged by integration of the ^1H NMR spectrum. ^1H NMR (300 MHz, CD_3CN) δ: 14.98 (d, $^3J_{HP}$ = 0.8 Hz, 1H, C*H*O), 7.37−7.80 (m, 14H, Ar*H*, overlapped with PPN^+), 3.63 (m, THF, overlapped with **W^0**), 3.02 (s, 2H, CH_2), 1.78 (s, 6H, CH_3), 1.78 (m, THF, overlapped with previous peak). $^{13}C\{^1H\}$ NMR (126 MHz, CD_3CN): 259.6 (d, $^2J_{CP}$ = 9.4 Hz, CHO), 190.7 (d, $^2J_{CP}$ = 7.3 Hz, cis CO), 190.5 (d, $^2J_{CP}$ = 9.5 Hz, cis CO), 188.1 (d, $^2J_{CP}$ = 43.7 Hz, trans CO), 143.8 (d, J_{CP} = 6.0 Hz, Ar), 135.4 (d, J_{CP} = 13.3 Hz, Ar), 134.9 (s, Ar), 134.1 (d, J_{CP} = 11.3 Hz, Ar), 132.2 (d, J_{CP} = 2.3 Hz, Ar), 131.9 (d, J_{CP} = 2.4 Hz, Ar), 131.2 (d, J_{CP} = 7.6 Hz, Ar), 131.2 (s, Ar), 129.9 (d, J_{CP} = 10.4 Hz, Ar), 127.8 (d, J_{CP} = 13.7 Hz, Ar), 68.3 (s, THF), 63.2 (d, J_{CP} = 4.7 Hz, CH_2), 45.3 (s, CH_3), 26.2 (s, THF). $^{31}P\{^1H\}$ NMR (121 MHz,

dx.doi.org/10.1021/om400810v | *Organometallics* 2013, 32, 5530−5545

CD_3CN) δ: 11.6. IR (CH_3CN): $\tilde{\nu}_{C\equiv O}$ = 2090 (m), 1994 (sh), 1984 (s), 1964 (s) cm^{-1}; $\tilde{\nu}_{C=O}$ = 1590 (m) cm^{-1}.

Preparation of *cis*-Re^{I}(L3-κ_1-P)(CO)$_4$(CHO) (18). Following the described procedure, complex **18** was prepared from **3** (25 mg, 0.036 mmol) and **W−H** (38 mg, 0.040 mmol, 1.1 equiv), forming in ca. 85% yield as judged by integration of the ^{1}H NMR spectrum, with *cis*-Re^{I}(**L3**-κ_1-P)(CO)$_4$(H) as the major side product. ^{1}H NMR (300 MHz, CD_3CN) δ: 15.14 (s, 1H, C*H*O), 7.40−7.80 (m, 10H, Ar*H*, overlapped with PPN$^+$), 3.60 (d, $^2J_{HP}$ = 3.7 Hz, 2H, CH_2), 3.41 (m, 4H, CH_2), 2.15 (app. t, J = 4.6 Hz, 4H, CH_2). ^{13}C{^{1}H} NMR (126 MHz, CD_3CN) δ: 259.2 (d, $^2J_{CP}$ = 10.4 Hz, CHO), 190.5 (d, $^2J_{CP}$ = 7.8 Hz, cis CO), 190.1 (d, $^2J_{CP}$ = 9.5 Hz, cis CO), 188.9 (d, $^2J_{CP}$ = 43.4 Hz, trans CO), 133.8 (s, Ar), 133.6 (d, J_{CP} = 9.9 Hz, Ar), 132.0 (s, Ar), 129.8 (d, J_{CP} = 9.6 Hz, Ar), 67.1 (s, CH_2), 59.7 (d, J_{CP} = 45.4 Hz, CH_2), 59.2 (d, J_{CP} = 6.8 Hz, CH_2). ^{31}P{^{1}H} NMR (121 MHz, CD_3CN) δ: 6.7. IR (CH_3CN): $\tilde{\nu}_{C\equiv O}$ = 2080 (m), 1993 (sh), 1983 (s), 1953 (s) cm^{-1}; $\tilde{\nu}_{C=O}$ = 1590 (m) cm^{-1}.

Preparation of *cis*-Re^{I}(L4-κ_1-P)(CO)$_4$(CHO) (19). Following the general procedure, complex **19** was prepared in ca. 85% yield from **4** (25 mg, 0.032 mmol) and **W−H** (31 mg, 0.032 mmol, 1.0 equiv). ^{1}H NMR (300 MHz, CD_3CN) δ: 14.86 (d, $^3J_{HP}$ = 1.4 Hz, 1H, C*H*O), 7.27−7.80 (m, 12H, Ar*H*, overlapped with PPN$^+$), 6.91 (ddd, J = 9.0, 5.3, 2.3 Hz, 1H, Ar*H*), 6.33 (m, 1H, Ar*H*), 2.20 (s, 12H, CH_3). ^{13}C{^{1}H} NMR (126 MHz, CD_3CN) δ: 260.0 (d, $^2J_{CP}$ = 9.6 Hz, CHO), 191.8 (d, $^2J_{CP}$ = 8.0 Hz, cis CO), 191.2 (d, $^2J_{CP}$ = 9.7 Hz, cis CO), 189.2 (d, $^2J_{CP}$ = 42.0 Hz, trans CO), 159.6 (s, C═N), 155.3 (d, J_{CP} = 2.8 Hz, Ar), 136.8 (d, J_{CP} = 15.7 Hz, Ar), 134.5 (d, J_{CP} = 50.8 Hz, Ar), 133.6 (d, J_{CP} = 11.0 Hz, Ar), 133.6 (s, Ar), 130.7 (d, J_{CP} = 2.3 Hz, Ar), 128.8 (d, J_{CP} = 10.2 Hz, Ar), 122.3 (d, J_{CP} = 5.4 Hz, Ar), 119.4 (d, J_{CP} = 12.4 Hz, Ar), 119.0 (s, Ar), 39.4 (s, CH_3). ^{31}P{^{1}H} NMR (121 MHz, CD_3CN) δ: 9.3. IR (CH_3CN): $\tilde{\nu}_{C\equiv O}$ = 2086 (m), 1982 (s), 1958 (s) cm^{-1}; $\tilde{\nu}_{C=O}$ = 1590 (m) cm^{-1}.

Preparation of *cis*-Re^{I}(L5-κ_1-P)(CO)$_4$(CHO) (20). In a slight departure from the typical procedure, protonated complex **12** (25 mg, 0.030 mmol) was combined with **W−H** (60 mg, 0.062 mmol, 2.1 equiv) to form **20** in ca. 50% yield. Alternatively, treatment of **5** (contaminated with ca. 15% **7**) with 1 equivalent of **W−H** gave complex **20** in similar yields. ^{1}H NMR (300 MHz, CD_3CN) δ: 15.16 (d, $^3J_{HP}$ = 1.1 Hz, 1H, C*H*O), 7.30−7.80 (m, 10H, Ar*H*, overlapped with PPN$^+$), 2.80−3.95 (m, 7H, C*H* + CH_2), 1.25−2.15 (m, 8H, CH_2). ^{31}P{^{1}H} NMR (121 MHz, CD_3CN) δ: 8.9 (br). IR (CH_3CN): $\tilde{\nu}_{C\equiv O}$ = 2080 (m), 1985 (s) cm^{-1}; $\tilde{\nu}_{C=O}$ = 1589 (m) cm^{-1}.

Preparation of (Li$^+$)[*cis*-Re^{I}(L6$^-$-κ_1-P)(CO)$_4$(CHO)]$^-$ (21). Complex **6**·CH_2Cl_2 (25 mg, 0.030 mmol) was dissolved in 0.7 mL of CD_3CN. To the resulting colorless solution was added $LiHBEt_3$ solution (1.0 M, 75 μL, 0.075 mmol, 2.5 equiv), which yielded a yellow solution containing BEt_3-stabilized **21** in ca. 75% yield. ^{1}H NMR (300 MHz, CD_3CN) δ: 15.14 (d, $^3J_{HP}$ = 1.7 Hz, 1H, C*H*O), 7.18−7.60 (m, 10H, Ar*H*), 7.01 (d, J = 2.4 Hz, 1H, Ar*H*), 5.82 (m, 1H, Ar*H*), 1.93 (s, 3H, ArCH_3), 1.41 (s, 9H, C(CH_3)$_3$). ^{13}C{^{1}H} NMR (126 MHz, CD_3CN) δ: 274.9 (d, $^2J_{CP}$ = 12.0 Hz, CHO), 191.6 (d, $^2J_{CP}$ = 7.6 Hz, cis CO), 189.2 (d, $^2J_{CP}$ = 41.4 Hz, trans CO),[47] 169.3, (d, J_{CP} = 7.8 Hz, Ar), 139.6 (d, J_{CP} = 5.4 Hz, Ar), 135.0 (s, Ar), 134.9 (s, Ar), 131.6 (s, Ar), 130.5 (s, Ar), 130.3 (d, J_{CP} = 7.8 Hz, Ar), 129.0 (d, J_{CP} = 9.9 Hz, Ar), 118.7 (d, J_{CP} = 11.6 Hz, Ar), 115.9 (d, J_{CP} = 62.1 Hz, Ar), 35.4 (s, C(CH_3)$_3$), 30.2 (s, C(CH_3)$_3$), 21.2 (s, ArCH_3). ^{31}P{^{1}H} NMR (121 MHz, CD_3CN) δ: 5.6. IR (CH_3CN): $\tilde{\nu}_{C\equiv O}$ = 2088 (m), 1998 (s), 1968 (s), 1948 (s) cm^{-1}; $\tilde{\nu}_{C=O}$ = 1584 (m) cm^{-1}.

Preparation of *cis*-[Re^{I}(L2H-κ_1-P)(CO)$_4$(CHO)](BF$_4$) (22). Complex **17** was prepared as described above, at the same scale and housed in a J. Young NMR tube. After 15 min, the tube was frozen in the glovebox cold well. Pyridinium tetrafluoroborate (5.2 mg, 0.031 mmol, 1.0 equiv) was added to the frozen solution from a stock solution. The tube was allowed to thaw while sealed, and the NMR spectra were recorded immediately, indicating the presence of the desired product in ca. 50% yield. ^{1}H NMR (300 MHz, CD_3CN) δ: 15.15 (br, s, 1H, C*H*O), 7.15−7.80 (m, 14H, Ar*H*, overlapped with PPN$^+$), 3.05 (br, s, 2H, CH_2), 2.29 (br, s, 6H, CH_3). ^{31}P{^{1}H} NMR (121 MHz, CD_3CN) δ: 13.0. IR (CH_3CN): $\tilde{\nu}_{C\equiv O}$ = 2097 (m), 1983 (s), 1964 (sh) cm^{-1}; $\tilde{\nu}_{C=O}$ = 1590 (w) cm^{-1}. The low yield of the reaction and poor stability of the product precluded ^{13}C{^{1}H} NMR determination, which showed very broad features in an initial attempt to collect.

Preparation of *cis*-[Re^{I}(L4H-κ_1-P)(CO)$_4$(CHO)](BF$_4$) (23). Complex **19** was prepared as described above. After 15 min, the solution was frozen in the glovebox cold well. The frozen solution was removed, and upon thawing 2,6-lutidinium tetrafluoroborate (5.7 mg, 0.029 mmol, 0.90 equiv) was delivered from a stock solution. The solution was transferred to a J. Young NMR tube, which was sealed. The initial NMR spectra indicate the desired product present in 70% yield. ^{1}H NMR (300 MHz, CD_3CN) δ: 15.38 (br, s, 1H, C*H*O), 9.23 (s, 1H, N*H*), 6.98−7.80 (m, 14H, Ar*H*, overlapped with PPN$^+$ and 2,6-lutidine), 2.73 (br, s, 12H, CH_3). ^{13}C{^{1}H} NMR (126 MHz, CD_3CN) δ: 269.4 (d, $^2J_{CP}$ = 9.4 Hz, CHO), 189.5 (d, $^2J_{CP}$ = 7.7 Hz, cis CO), 189.1 (d, $^2J_{CP}$ = 6.8 Hz, cis CO), 187.4 (d, $^2J_{CP}$ = 45.0 Hz, trans CO), 159.3 (s, C═N), 158.6 (s, Ar), 140.9 (s, Ar), 138.6 (s, Ar), 137.0 (d, J_{CP} = 11.9 Hz, Ar), 134.9 (s, Ar), 133.1 (d, J_{CP} = 4.6 Hz, Ar), 127.4 (d, J_{CP} = 9.7 Hz, Ar), 126.9 (s, Ar), 124.8 (s, Ar), 121.7 (s, Ar), 41.4 (s, CH_3). ^{31}P{^{1}H} NMR (121 MHz, CD_3CN) δ: 10.5. IR (CH_3CN): $\tilde{\nu}_{C\equiv O}$ = 2095 (m), 2008 (sh), 1988 (s) cm^{-1}; $\tilde{\nu}_{C=O}$ = 1580[48] (w) cm^{-1}.

Preparation of *cis*-Re^{I}(L6-κ_1-P)(CO)$_4$(CHO) (24). Complex **21** was prepared as described above, in 0.4 mL of CD_3CN. The solution was frozen in the glovebox cold well. The frozen solution was removed and allowed to thaw, and 2,6-lutidinium tetrafluoroborate (7.0 mg, 0.036 mmol, 1.2 equiv) in 0.3 mL of CD_3CN was added while still cold. The solution was transferred to a J. Young NMR tube, and initial NMR spectra indicated the desired product present in 75% yield. ^{1}H NMR (300 MHz, CD_3CN) δ: 14.82 (s, 1H, C*H*O), 8.42 (s, 1H, O*H*), 7.36−7.64 (m, 10H, Ar*H*, overlapped with 2,6-lutidine), 7.32 (d, J = 2.2 Hz, 1H, Ar*H*), 6.45 (dd, J = 11.8, 2.1 Hz, 1H, Ar*H*), 2.11 (s, 3H, ArCH_3), 1.41 (s, 9H, C(CH_3)$_3$). ^{31}P{^{1}H} NMR (121 MHz, CD_3CN) δ: 7.6. IR (CH_3CN): $\tilde{\nu}_{C\equiv O}$ = 2095 (m), 1986 (s), 1938 (m) cm^{-1}; $\tilde{\nu}_{C=O}$ = 1595 (w) cm^{-1}.

General Procedure for pK_a Determination. The pK_a of **L1** has been previously determined.[20] All new pK_a values reported here were determined by NMR spectroscopy and are the average of two or more self-consistent trials. The compound of interest was combined with an acid or base with a known pK_a, and the equilibrium populations were determined by NMR. In most cases, proton transfer was rapid on the NMR time scale, in which case the equilibrium concentration was determined from the chemical shift, using the equation $\chi_A = (\delta_{eq} - \delta_B)/(\delta_A - \delta_B)$, where χ_A is the mole fraction of the conjugate acid, and δ refers to the measured chemical shift of a given peak at equilibrium (eq) and for pure samples of the conjugate acid (A) and base (B). The value of χ_A was determined using all well-resolved ^{1}H NMR signals, as well as from the ^{31}P{^{1}H} spectrum. Good agreement between the independent calculations of χ_A was obtained, and the value used to calculate the equilibrium concentration was an average of the independently determined values. In some cases, particularly for rhenium pentacarbonyl complexes, the equilibration between the acidic and basic forms of the complex was slow, in which case distinct peaks for the two species could be resolved and concentrations were determined by NMR integration. Once the equilibrium concentrations were determined, the equilibrium constant for the reaction between the compound of interest and the known acid/base was determined, and by using Hess's law the pK_a of the compound was calculated. For the pK_a measurements of the formyl complexes, minor side reactions consumed some of the added acid. Thus for these experiments the ratios of the conjugate acid and base for both the rhenium formyl complex and the known acid were determined independently from the equilibrium NMR spectrum, allowing K_{eq} to be more accurately determined.

The following acids/bases were used for determination of unknown pK_a values: triethylamine (pK_a = 18.82) for **L2H** and **L3H**; 2-(2′-tolyl)-1,1,3,3-tetramethylguanidine (pK_a = 20.5)[30] for **L4H**; DBU (pK_a = 24.34)[31] for **L5H**; phenol (pK_a = 28.12) for **L6**; pyridine (pK_a = 12.53)[31] for **8**, **9**, and **11**; 2-chloroaniline (pK_a = 7.86) for **10**; 2,6-lutidine and 2,6-lutidinium (pK_a = 14.13) for **12** and **22**, respectively; DMAP (pK_a = 17.95)[31] for **6**; and DMAPH$^+$ for **23** and **24**.

dx.doi.org/10.1021/om400810v | *Organometallics* 2013, 32, 5530−5545

X-ray Crystallographic Procedures. All crystallizations were carried out at room temperature. Crystals of (**L5H**)(BF_4) were obtained from 2-butanone at room temperature, **1** was crystallized from a mixture of CH_2Cl_2 and chlorobenzene by vapor diffusion of THF, **2**, **3**, and **6**–**9** were crystallized from MeCN by vapor diffusion of Et_2O, **4** was crystallized from CH_2Cl_2 layered with Et_2O, crystals of **11** were grown from CH_2Cl_2/MeCN by diffusion of Et_2O, and crystals of **12** deposited from MeCN by vapor diffusion of CH_2Cl_2. Crystals were mounted on either a Bruker APEXII four-circle diffractometer or Bruker three-circle diffractometer with a SMART 1K CCD detector using Mo radiation from a sealed-tube 3 kW X-ray generator. The data were collected at 100(2) K and were processed and refined using the program SAINT supplied by Siemens Industrial Automation. Structures were solved by Patterson methods or direct methods in SHELXS and refined by standard difference Fourier techniques in the SHELXTL program suite (6.10 v., Sheldrick G. M., and Siemens Industrial Automation, 2000). Hydrogen atoms bonded to carbon were placed in calculated positions using the standard riding model and refined isotropically; all non-hydrogen atoms were refined anisotropically. In the structures of (**L5H**)(BF_4), **6**–**9**, **11**, and **12**, oxygen and nitrogen-bound hydrogen atoms were located in the difference map, restrained to a distance of 0.84 Å (O–H) or 0.88 Å (N–H), and refined isotropically with the isotropic displacement parameter constrained to be 1.2 times greater than that of the atom it is bonded to. In the structures of **1** and **4**, BF_4^- counterions were found to be disordered about two positions. For the disordered parts, bond distances and angles were restrained to be similar using the "SADI" command, and the rigid bond restraints "SIMU" and "DELU" were also employed. The structure of **4** also contained a solvent molecule disordered about a cubic special position. The size and electron density of this void was consistent with the presence of a single Et_2O solvent molecule, but the electron density could not be satisfactorily modeled. The SQUEEZE function within PLATON was employed for the final refinement cycles of this structure. A summary of crystallographic details for all structures is provided in Tables S1–S4 in the Supporting Information.

■ ASSOCIATED CONTENT

Ⓢ Supporting Information

Crystallographic summary tables, X-ray crystal structure depictions for (**L5H**)(BF_4), **1**–**3**, **6**, **7**–**9**, and **12**, NMR spectra for all new compounds. This material is available free of charge via the Internet at http://pubs.acs.org.

■ AUTHOR INFORMATION

Corresponding Authors

*E-mail (J. E. Bercaw): bercaw@caltech.edu.

*E-mail (J. A. Labinger): jal@caltech.edu

Notes

The authors declare no competing financial interest.

■ ACKNOWLEDGMENTS

We thank BP for their support of this work through the XC^2 program.

■ REFERENCES

(1) Keim, W. "Synthesis Gas." In *Industrial Chemicals via C1 Processes*; Fahey, D. R., Ed.; American Chemical Society: Washington, DC, 1987; Vol. *328*, pp 1–16.

(2) (a) Rofer-DePoorter, C. K. *Chem. Rev.* **1981**, *81*, 447–474. (b) Khodakov, A. Y.; Chu, W.; Fongarland, P. *Chem. Rev.* **2007**, *107*, 1692–1744.

(3) Fischer, F.; Tropsch, H. Process for the Production of Paraffin-Hydrocarbons with More Than One Carbon Atom. U.S. Patent 1,746,464, February 11, 1930.

(4) De Smit, E.; Weckhuysen, B. M. *Chem. Soc. Rev.* **2008**, *37*, 2758–2781.

(5) (a) den Breejen, J. P.; Radstake, P. B.; Bezemer, G. L.; Bitter, J. H.; Frøseth, V.; Holmen, A.; de Jong, K. P. *J. Am. Chem. Soc.* **2009**, *131*, 7197–7203. (b) Borg, O.; Dietzel, P. D. C.; Spjelkavik, A. I.; Tveten, E. Z.; Walmsley, J. C.; Diplas, S.; Eri, S.; Holmen, A.; Rytter, E. *J. Catal.* **2008**, *259*, 161–164. (c) Torres Galvis, H. M.; Koeken, A. C. J.; Bitter, J. H.; Davidian, T.; Ruitenbeek, M.; Dugulan, A. I.; de Jong, K. P. *J. Catal.* **2013**, *303*, 22–30. (d) Dinse, A.; Aigner, M.; Ulbrich, M.; Johnson, G. R.; Bell, A. T. *J. Catal.* **2012**, *288*, 104–114.

(6) (a) Gong, J.; Yue, H.; Zhao, Y.; Zhao, S.; Zhao, L.; Lv, J.; Wang, S.; Ma, X. *J. Am. Chem. Soc.* **2012**, *134*, 13922–13925. (b) Yin, H.; Ding, Y.; Luo, H.; Yan, L.; Wang, T.; Lin, L. *Energy Fuels* **2003**, *17*, 1401–1406.

(7) (a) Loveless, B. T.; Buda, C.; Neurock, M.; Iglesia, E. *J. Am. Chem. Soc.* **2013**, *135*, 6107–6121. (b) Ojeda, M.; Li, A.; Nabar, R.; Nilekar, A. U.; Mavrikakis, M.; Iglesia, E. *J. Phys. Chem. C* **2010**, *114*, 19761–19770.

(8) (a) De Smit, E.; Cinquini, F.; Beale, A. M.; Safonova, O. V.; van Beek, W.; Sautet, P.; Weckhuysen, B. M. *J. Am. Chem. Soc.* **2010**, *132*, 14928–14941. (b) Zhao, Y.-F.; Rousseau, R.; Li, J.; Mei, D. *J. Phys. Chem. C* **2012**, *116*, 15952–15961.

(9) West, N. M.; Miller, A. J. M.; Labinger, J. A.; Bercaw, J. E. *Coord. Chem. Rev.* **2011**, *255*, 881–898.

(10) (a) Demitras, G. C.; Muetterties, E. L. *J. Am. Chem. Soc.* **1977**, *99*, 2796–2797. (b) Collman, J. P.; Brauman, J. I.; Tustin, G.; Wann, G. S., III. *J. Am. Chem. Soc.* **1983**, *105*, 3913–3922.

(11) (a) Dombek, B. D. *Adv. Catal.* **1983**, *32*, 325–416. (b) Kiso, Y.; Tanaka, M.; Hayashi, T.; Saeki, K. *J. Organomet. Chem.* **1987**, *322*, C32–C36.

(12) (a) Gladysz, J. A. *Adv. Organomet. Chem.* **1982**, *20*, 1–38. (b) Collman, J. P.; Winter, S. R. *J. Am. Chem. Soc.* **1973**, *95*, 4089–4090. (c) Casey, C. P.; Andrews, M. A.; Rinz, J. E. *J. Am. Chem. Soc.* **1979**, *101*, 741–743. (d) Tam, W.; Wong, W.-K.; Gladysz, J. A. *J. Am. Chem. Soc.* **1979**, *101*, 1589–1591. (e) Barger, P. T.; Bercaw, J. E. *Organometallics* **1984**, *3*, 278–284.

(13) Wolczanski, P. T.; Bercaw, J. E. *Acc. Chem. Res.* **1980**, *13*, 121–127.

(14) (a) Butts, S. B.; Holt, E. M.; Strauss, S. H.; Alcock, N. W.; Stimson, R. E.; Shriver, D. F. *J. Am. Chem. Soc.* **1979**, *101*, 5864–5866. (b) Lindner, E.; von Au, G. *Angew. Chem., Int. Ed. Engl.* **1980**, *19*, 824–825.

(15) (a) Miller, A. J. M.; Labinger, J. A.; Bercaw, J. E. *J. Am. Chem. Soc.* **2008**, *130*, 11874–11875. (b) Miller, A. J. M.; Labinger, J. A.; Bercaw, J. E. *J. Am. Chem. Soc.* **2010**, *132*, 3301–3303. (c) Miller, A. J. M.; Labinger, J. A.; Bercaw, J. E. *Organometallics* **2010**, *29*, 4499–4516.

(16) Dobrovetsky, R.; Stephan, D. W. *J. Am. Chem. Soc.* **2013**, *135*, 4974–4977.

(17) Sazama, G. T.; Betley, T. A. *Organometallics* **2011**, *30*, 4315–4319.

(18) (a) West, N. M.; Labinger, J. A.; Bercaw, J. E. *Organometallics* **2011**, *30*, 2690–2700. (b) Hazari, A.; Labinger, J. A.; Bercaw, J. E. *Angew. Chem., Int. Ed.* **2012**, *51*, 8268–8271.

(19) Ellis, W. W.; Miedaner, A.; Curtis, C. J.; Gibson, D. H.; DuBois, D. L. *J. Am. Chem. Soc.* **2002**, *124*, 1926–1932.

(20) Farrer, N. J.; McDonald, R.; McIndoe, J. S. *Dalton Trans.* **2006**, 4570–4579.

(21) (a) Rauchfuss, T. B.; Patino, F. T.; Roundhill, D. M. *Inorg. Chem.* **1975**, *14*, 652–656. (b) Alonso, M. A.; Casares, J. A.; Espinet, P.; Soulantica, K.; Orpen, A. G.; Phetmung, H. *Inorg. Chem.* **2003**, *42*, 3856–3864.

(22) Song, H.-B.; Zhang, Z.-Z.; Mak, T. C. W. *New J. Chem.* **2002**, *26*, 113–119.

(23) O'Reilly, M.; Pattacini, R.; Braunstein, P. *Dalton Trans.* **2009**, 6092–6095.

(24) Matsumura, N.; Nishiguchi, H.; Okada, M.; Yoneda, S. *J. Heterocycl. Chem.* **1986**, *23*, 885–887.

(25) Rauchfuss, T. B. *Inorg. Chem.* **1977**, *16*, 2966–2968.

(26) Haddad, M.; Laghzaoui, M.; Welter, R.; Dagorne, S. *Organometallics* **2009**, *28*, 4584–4592.

(27) Pruszynski, P. *Can. J. Chem.* **1987**, *65*, 626–629.

(28) Beck, W.; Raab, K.; Shapley, J. R.; Whittlesey, B. R. *Inorg. Synth.* **1989**, *26*, 106−113.
(29) Drew, D.; Darensbourg, D. J.; Darensbourg, M. Y. *Inorg. Chem.* **1975**, *14*, 1579−1584.
(30) Leffek, K. T.; Pruszynski, P.; Thanapaalasingham, K. *Can. J. Chem.* **1989**, *67*, 590−595.
(31) Kaljurand, I.; Kütt, A.; Sooväli, L.; Rodima, T.; Mäemets, V.; Leito, I.; Koppel, I. A. *J. Org. Chem.* **2005**, *70*, 1019−1028.
(32) Kütt, A.; Movchun, V.; Rodima, T.; Dansauer, T.; Rusanov, E. B.; Leito, I.; Kaljurand, I.; Koppel, J.; Pihl, V.; Koppel, I.; Ovsjannikov, G.; Toom, L.; Mishima, M.; Medebielle, M.; Lork, E.; Röschenthaler, G.-V.; Koppel, I. A.; Kolomeitsev, A. A. *J. Org. Chem.* **2008**, *73*, 2607−2620.
(33) Slater, S. G.; Lusk, R.; Schumann, B. F.; Darensbourg, M. *Organometallics* **1982**, *1*, 1662−1666.
(34) Ellis, W. W.; Ciancanelli, R.; Miller, S. M.; Raebiger, J. W.; Rakowski DuBois, M.; DuBois, D. L. *J. Am. Chem. Soc.* **2003**, *125*, 12230−12236.
(35) Schenk, W. A. *J. Organomet. Chem.* **1979**, *179*, 253−261.
(36) One of the bands appears as a shoulder and was not resolved in the spectra of **19** and **20**.
(37) (a) Henry, R. M.; Shoemaker, R. K.; DuBois, D. L.; Rakowski DuBois, M. *J. Am. Chem. Soc.* **2006**, *128*, 3002−3010. (b) Stephan, D. W.; Erker, G. *Angew. Chem., Int. Ed.* **2010**, *49*, 46−76.
(38) Elowe, P. R.; West, N. M.; Labinger, J. A.; Bercaw, J. E. *Organometallics* **2009**, *28*, 6218−6227.
(39) Pangborn, A. B.; Giardello, M. A.; Grubbs, R. H.; Rosen, R. K.; Timmers, F. J. *Organometallics* **1996**, *15*, 1518−1520.
(40) Long, R. J.; Gibson, V. C.; White, A. J. P.; Williams, D. J. *Inorg. Chem.* **2006**, *45*, 511−513.
(41) Golisz, S. R.; Bercaw, J. E. *Macromolecules* **2009**, *42*, 8751−8762.
(42) Schmidt, S. P.; Nitschke, J.; Trogler, W. C.; Huckett, S. I.; Angelici, R. J. *Inorg. Synth.* **1989**, *26*, 113−117.
(43) Perrin, D. D. *Purification of Laboratory Chemicals*, 3rd ed.; Pergamon Press: Oxford, 1988.
(44) Miedaner, A.; DuBois, D. L.; Curtis, C. J.; Haltiwanger, R. C. *Organometallics* **1993**, *12*, 299−303.
(45) The $^{13}C\{^{1}H\}$ spectrum was broad, and only six of the expected 10 aromatic signals were resolved.
(46) Lacour, M.-A.; Zablocka, M.; Duhayon, C.; Majoral, J.-P.; Taillefer, M. *Adv. Synth. Catal.* **2008**, *350*, 2677−2682.
(47) The third CO resonance in the $^{13}C\{^{1}H\}$ NMR was not located, but all other spectroscopic data are consistent with the stated formulation.
(48) The presence of ligand stretches in this region made it difficult to precisely locate the weak C═O stretch.